Methods for online voltage stability monitoring

by

Mahesh Jung Karki

A thesis submitted to the graduate faculty

in partial fulfillment of the requirements for the degree of

MASTER OF SCIENCE

Major: Electrical Engineering

Program of Study Committee:
Venkataramana Ajjarapu, Major Professor
Dionysios Aliprantis
Sigurdur Olafsson

Iowa State University

Ames, Iowa

2009

TABLE OF CONTENTS

LIST OF TABLES

LIST OF FIGURES

1 INTRODUCTION

1.1 Overview

Severe and increasing strain has been observed in the power system in recent years due to incongruence between the generation and transmission infrastructure. Environmental issues, change in energy portfolio and deregulated energy markets are some of the prime factors. The kind of stress developed in the system has caused concerns for voltage instability. Voltage stability refers to the ability of a power system to maintain steady voltages at all buses in the system after being subjected to a disturbance from a given initial operating condition [1]. It is very closely related to load dynamics [2].There are several studies [3,4,5,6] focused on measures to accurately predict system conditions with respect to voltage stability and optimal control actions to avoid collapse in the online paradigm. As most of these problems are highly nonlinear and computationally intensive, there is a need of research to help in reducing computation and using direct measurements for estimation of stability margin.

Table 1.1 lists some severe voltage instability incidents over the past half century [7]. These events cause loss of billions of dollars. Due to such high frequency of voltage instability events there is a serious concern for remedial measures. Online voltage stability monitoring is an effort towards mitigation of such system wide voltage stability events. The tabulation is done in terms of time frame of instability. The events have been classified as long term and short term. The generic details of the mechanics of these long term and short term events are described in Chapter 2.

Table 1.1 Voltage stability incidents

Date	Location	Time Frame
April 13 1986	Winnipeg, Canada Nelson River HVDC link	Short term, 1 sec
Nov. 30 1986	SE Brazil, Paraguay, Itaipu HVDC link	Short term, 2 sec
May 17 1985	South Florida, USA	Short term,4 sec
Dec. 27, 1983	Sweden	Long term,55sec
Dec. 30, 1982	Florida, USA	Long term,1-3 min
Sept. 22,1977	Jacksonville, Florida	Long term, few min
Aug. 4, 1982	Belgium	Long term,4-5 min
Nov. 10,1976	Brittany, France	Long term
July 23, 1987	Tokyo, Japan	Long term, 20 min
Dec. 19,1978	France	Long term, 26 min
Aug. 22,1970	Japan	Long term, 30 min

1.2 Scope of Work

The goal of this thesis is to elaborate on the methods of online voltage stability monitoring. Online voltage stability monitoring is the process of obtaining voltage stability information for a given operating scenario. The prediction should be fast and accurate such that control signals can be sent to appropriate locations quickly and effectively.

One approach is to get the stability information directly from the phasor measurements obtained for operating conditions. This approach is simple and requires few computations. The methods proposed are based on Thévenin equivalent of a system [3]. The Thévenin equivalent, according to the maximum power transfer theorem, is the upper limit of the power transfer to a load bus. To get the Thévenin equivalent we need at

least two sets of phasor measurements [8]. It is found that Thévenin equivalent gives a highly optimistic approximation of power margin. The work done in this thesis compensates the optimistic prediction by applying reactive power availability information of the system.

In another approach, offline observations (either simulated results or stored measurements) are used to build a statistical model of the power system. The model takes measurements consisting of current state as the input and returns the voltage stability information as the output. The model is periodically updated as the power system evolves through time into different unanticipated states. Artificial intelligence methods such as expert systems [9, 10], decision trees (DTs) [11, 12, 13] and neural networks [14, 15] fall into this category. The use of decision trees is gaining popularity because of its simplicity and the structural insight they provide on the decision being made. This study is, thus, focused on improving the application of decision trees in power systems. This is accomplished by a new method for attribute selection based on the principles of power systems.

1.3 Thesis Outline

In Chapter 2, existing tools for voltage stability analysis are described and a brief introduction on the voltage stability problem is given. Chapter 3 reports state of the art methods for online voltage stability monitoring. Chapter 4 presents an analytical approach in determination of voltage stability margin using online measurements by consideration of reactive power availability. In Chapter 5, decision tree methodology in power system industry and attribute selection method based on tangent vector elements has been described in detail. Finally, Chapter 6 provides the conclusions and suggestions for future work.

2 ELEMENTS OF VOLTAGE STABILITY ANALYSIS

2.1 Overview

Voltage instability is a non-linear phenomenon. It is impossible to capture the phenomenon as a closed form solution. The instability is manifested once the network crosses the maximum deliverable power limit. There are various types of dynamics associated with the problem, the critical ones being, load dynamics, generator reactive power limits and contingencies in the form of element outages. Voltage instability is classified in terms of scale of disturbance (small and large) and in terms of time of response (short term and long term) [1].

In the following sections, different aspects of voltage instability problem and their respective roles are described.

2.2 PV Curves

The PV curve is a power voltage relationship at a bus [2]. Figure 2.1 is an illustration of a typical PV diagram. ‘V’ in the vertical axis represents the voltage at a particular bus while ‘P’ in the horizontal axis denotes the real power at the corresponding bus or an area of our interest. The solid horizontal nose-shaped curve is the network PV curve while the dotted parabolic curve is the load PV curve. The operating point is the intersection between the load and the network curves [2]. Load PV curve shows the variation of power consumed by a load at a bus with respect to voltage applied to the load which depends upon the load characteristics. The commonly referred PV curve is the network PV curve. It is the network voltage response at a particular bus due to load increase in a certain area or bus of a power system. As the system moves from one

operating point to another, constant power characteristics and power factor of the load is assumed. The top half of the curve is the stable solution while the bottom half is unstable (determined by load characteristics but deemed unfeasible for power system operation due to high current and low voltage). The two solutions coalesce at a point called the critical point (also referred as, the nose point or the point of maximum power transfer). Beyond this point, the power flow does not converge. There are number of factors such as the generator reactive power limit, contingences, load dynamics, stress direction, etc that affect the distance of the nose point from the point of operation. By understanding these factors the system can be steered away from the nose point and make the system stable.

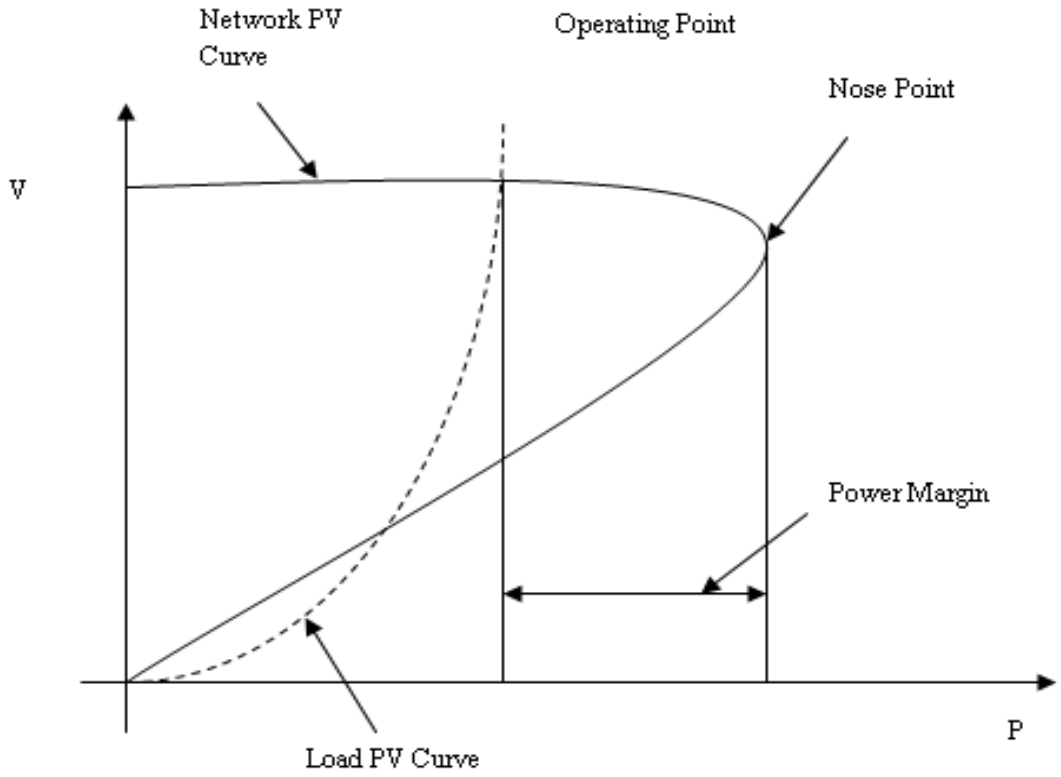

Figure 2.1 Load and network PV curves

2.2.1 PV Curve Tracing

PV curve tracing is computationally intensive and requires proper techniques to avoid numerical instability. For a simple two bus system, a closed form expression can be developed [2]. A series of network PV curves (for varying power factor) has been drawn using this expression in Figure 2.2. Although the curves are for a two bus system, the shapes are quite general.

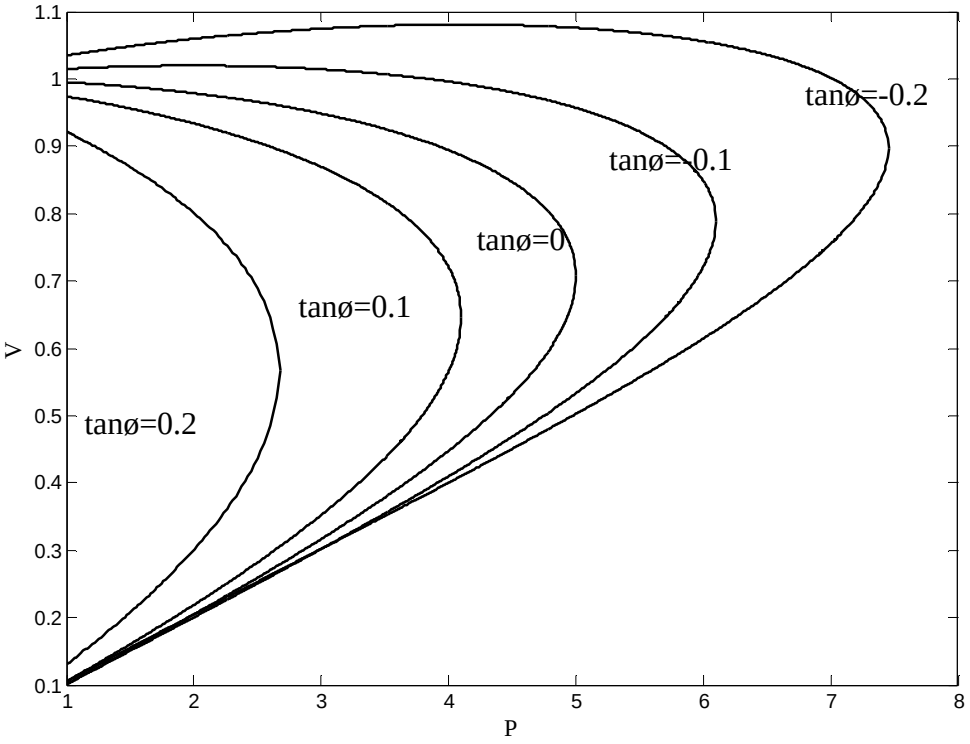

Figure 2.2 PV curves for different power factors

A closed form expression for voltage and power in large systems (systems with more than two buses) is not possible. In such a case, the technique is to solve the power flow equations numerically for each operating point. This makes the tracing highly computational. As the system gets closer to the nose point, getting convergence is

difficult. This is because, the power flow Jacobian approaches singularity towards the nose point and becomes singular when it is at the nose point. The singularity causes the power flow solution to diverge. Continuation power flow (CPF) [16] method is commonly used to solve the divergence problem.

2.2.1.1 Continuation Power Flow (CPF) Method

Equation 2.1 is the state-space representation of a power system.

$$\begin{aligned} \dot{\underline{x}} &= \underline{F}(\underline{x}, \underline{y}, \underline{p}) \\ \underline{0} &= \underline{G}(\underline{x}, \underline{y}, \underline{p}) \end{aligned} \tag{2.1}$$

This is a differential–algebraic system (DAS). In equation 2.1, $\underline{x}$ represents dynamic state variables of the system (mostly rotor angles, rotor speeds, torque, etc), $\underline{y}$ represents the algebraic state variables (usually bus voltage magnitudes and angles) and $\underline{p}$ represents the parameters (real and reactive power injections at each bus) appearing in $\underline{F}$ and $\underline{G}$. The function $\underline{F}$ denotes the differential equations for generators, tap changing transformers, etc and the function $\underline{G}$ represents the power flow equations.

The point at which the Jacobian of the system of equations 2.1 becomes singular is called bifurcation point. At this point, different branches of equilibrium points intersect each other. The Jacobian of equation 2.1 can be represented as follows:

$$\underline{J} = \begin{bmatrix} \underline{F_x} & \underline{F_y} \\ \underline{G_x} & \underline{G_y} \end{bmatrix} \tag{2.2}$$

Here, $\underline{G_y}$ is the power flow Jacobian. The singularity of $\underline{J}$ guarantees that the system goes into bifurcation while the singularity of $\underline{G_y}$ may or may not lead to bifurcation. The load level which produces a singular load flow Jacobian should be considered an optimistic upper bound on maximum loadability. For voltage collapse and voltage instability

analysis, any conclusion based on the singularity of the standard load-flow Jacobian would apply only to the phenomenon of voltage behavior near maximum power transfer. Such analysis would not detect any voltage instabilities associated with synchronous machine characteristics or their controls. G_y approaches singularity as the system loading is gradually increased. [17]

The CPF can be summarized using the flow chart shown in Figure 2.3. This is based on predictor- corrector process. From a known operating point, a prediction is made towards a more stressed condition by increase of the load parameter λ. Small enough steps should be taken such that the power flow at each step converges quickly. Corrector step succeeds predictor step. In corrector step, the solution of the power system at the predicted parameters is obtained. The requirement of the corrector step is to correct the linear prediction of non linear equations. For the correction step, a parameter called the continuation parameter is fixed. This step is crucial as it forces the system to come back to the solution. The process is repeated until we reach the critical point λ^*.

The ***Predictor step*** is used to determine the tangent vector. This is accomplished by solving equation 2.3.

$$\begin{bmatrix} \underline{G_\delta} & \underline{G_v} & \underline{G_\lambda} \end{bmatrix} \times \begin{bmatrix} d\underline{\delta} \\ d\underline{v} \\ d\lambda \end{bmatrix} = 0 \qquad 2.3$$

The matrix of derivatives in equation 2.3 is simply conventional power flow Jacobian augmented by one column ($\underline{G_\lambda}$) and $\underline{t}$ defined as, $\underline{t}=[d\underline{\delta} \quad d\underline{v} \quad d\underline{\lambda}]^T$ is the required tangent vector. After this, an appropriately dimensioned row vector is added with all elements equal to zero except the k^{th} element, which is set to 1. Proper choice of the index *k*, such that $t_k=\pm 1$ imposes a nonzero norm on the tangent vector and guarantees that the augmented Jacobian will be nonsingular at the critical point. Hence, the tangent vector is determined as the solution of equation 2.4.

$$\begin{bmatrix} \underline{G_\delta} & \underline{G_v} & \underline{G_\lambda} \\ & e_k & \end{bmatrix} \times \begin{bmatrix} d\underline{\delta} \\ d\underline{v} \\ d\underline{\lambda} \end{bmatrix} = \begin{bmatrix} 0 \\ \underline{+}1 \end{bmatrix} \quad 2.4$$

The next operating state is predicted as in equation 2.5.

$$\begin{bmatrix} \underline{\delta^*} \\ \underline{V^*} \\ \underline{\lambda^*} \end{bmatrix} = \begin{bmatrix} \underline{\delta} \\ \underline{V} \\ \underline{\lambda} \end{bmatrix} + \sigma \begin{bmatrix} d\underline{\delta} \\ d\underline{v} \\ d\underline{\lambda} \end{bmatrix} \quad 2.5$$

In equation 2.5, '*' denotes the predicted solution and 'σ' is a scalar designating step length.

The ***corrector step*** is accomplished by local parameterization; where original set of equations are augmented by an equation that specifies the value of one of the state variables called the continuation parameter. The simultaneous equations solved are as in equation 2.6.

$$\begin{bmatrix} G(\underline{x}) \\ x_k - \eta \end{bmatrix} = 0, \underline{x} = \begin{bmatrix} \underline{\delta} \\ \underline{V} \\ \underline{\lambda} \end{bmatrix} \quad 2.6$$

Where, η is an appropriate value for the k^{th} element of *x*.

Another approach for implementing the corrector step is the perpendicular step method. The additional equation is the condition that the vector connecting the corrected solution and the predicted solution should be perpendicular to the tangent vector. Thus the sets of equations to be solved are as in equation 2.7.

$$\begin{bmatrix} G(\underline{x}) \\ \{\underline{x^{i+1}} - \underline{x^{i+1,p}}\}.\underline{t} \end{bmatrix} = 0 \quad 2.7$$

Next, the continuation parameter is selected as in equation 2.8.

$$x_k : |t_k| = max\{|t_1|, |t_2|, \dots |t_3|\} \quad 2.8$$

Finally, the critical point is identified by checking the sign of $d\lambda$ component of the tangent vector. Positive value signifies upper portion of the PV curve, negative value

signifies the lower section of the curve and zero means the critical point. The tangent vector that is obtained as an intermediate step in continuation power flow contains sensitivity of the power flow parameters with respect to real power loading. This information is used in selecting the attributes in Chapter 5.

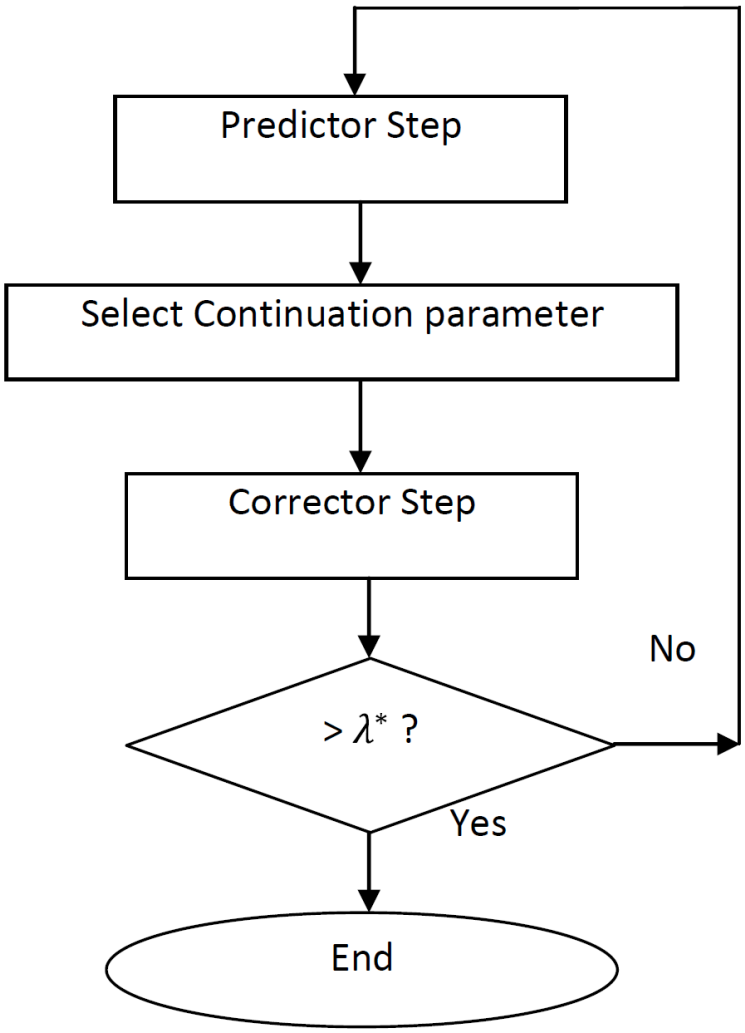

Figure 2.3 Flowchart for continuation power flow

2.3 QV Curves

QV curve is the relationship between the reactive support Q_c and the voltage at a given bus. It can be determined by connecting a fictitious generator with zero active power and recording the reactive power Q_c produced when the terminal voltage is varied [2].

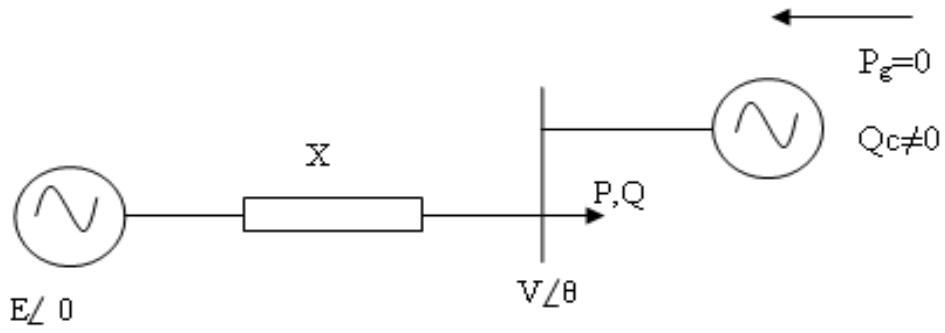

Figure 2.4 Setup to produce VQ curves

Considering the two bus examples as shown in Figure 2.4, the power flow equations are as shown in equations 2.9.

$$P = -\frac{EV}{X} sin\theta \qquad 2.9a.$$

$$Q - Q_c = -\frac{V^2}{X} + \frac{EV}{X} cos\theta \qquad 2.9b$$

VQ curve is a characteristic of both the network and load. For analysis of steady state operation, the steady state load characteristics needs to be considered. Here, a constant power load characteristic is assumed which is a common practice.

For a given value of real power (P) and voltage (V), θ is determined from equation 2.9a. Then Q_c can easily be determined from equation 2.9b - using the value of load reactive power and the variable determined from the first part. The result yields a QV curve similar to the ones shown in Figure 2.5. The minima of the curves indicate the available reactive power margin before the system goes to voltage collapse. As shown in the figure 2.5, the lengths of the arrows give the reactive power margin in terms of appropriate units. Curve 1 has negative margin. Thus there is no voltage level for which this system can be operated without some external reactive support. Curve 2 is a stable case with some reactive power margin and curve 3 has even more margin. More margin implies more robustness of the system in terms of voltage stability.

The right hand side of the QV curve with positive slope is the stable region and the left hand side of the QV curve with negative slope is the unstable region. They can be computed at points along the PV curves to test system robustness. There is no divergence at the nose. This makes the QV curve computationally attractive.

The nature of slope of the QV curves gives us indication of how different devices impact voltage stability of the system. For example, with generating units hitting the reactive power limits, the QV curve flattens out. This signifies the closeness to instability. With QV curves the characteristic of shunt reactive compensation at the test bus can be plotted [18]. The operating point is the intersection of the QV system characteristic and reactive compensation characteristic. This directly gives us the notion of reactive power margin and the current operating point, which is useful for planning and operation purposes.

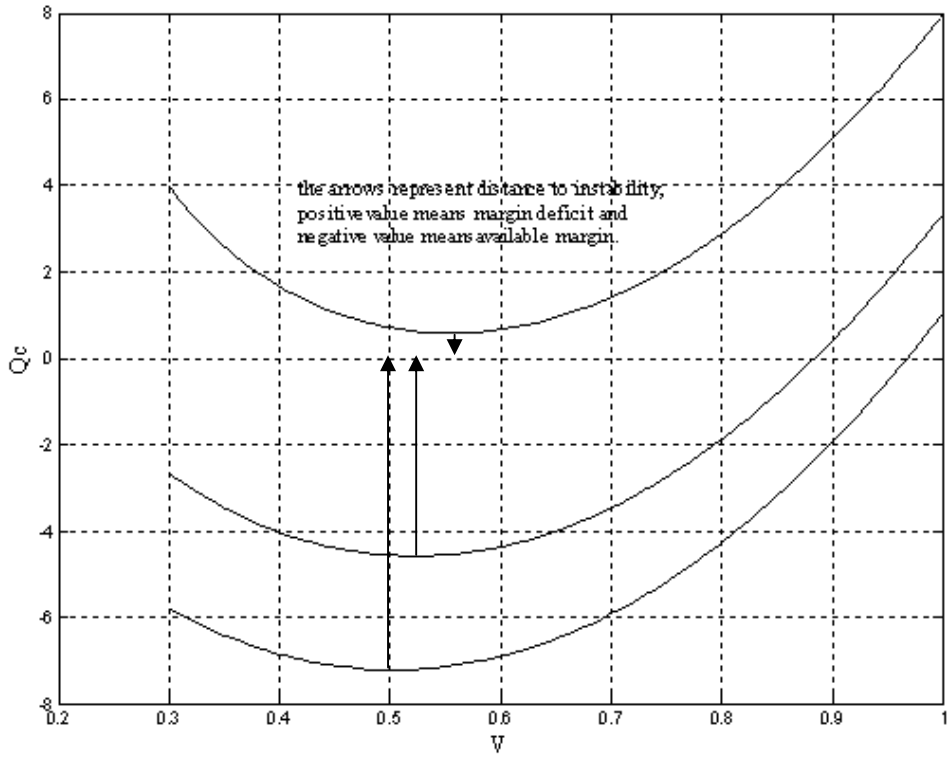

Figure 2.5 QV curves for different load levels

One of the information that can be accessed from the curves is the sensitivity of the loads to the reactive power sources. While varying the reactive power requirements of a bus, the generators that deplete their reactive reserves the most, form the reactive power sources for that bus. This quality of the QV curves has been used in the determination of voltage control area (VCA), as described in detail in Chapter 4.

2.4 Load Models and Dynamics

Load is an important factor of voltage instability. Load characteristics also govern the dynamic evolution of voltage instability. The point of voltage collapse can be different for different load models. Therefore, it is necessary to understand the load correctly and model it accordingly. At the same time it is a difficult task because bulk

power system is an aggregate of loads of varying characteristics. Another important aspect is the load restoration dynamics which includes slow and fast acting loads. Load restoration attributes to the fact that power system has the tendency to restore its voltage level through some of the devices, as load tap changers or voltage controller of generators and static reactive controllers. As a result, the load is restored to its original level by establishing the set point voltage in the final state. The power restoration can be fast as in the induction motors [7, 19], high voltage direct current (HVDC) links [2, 7] or slow as in the load tap changers (LTC) and thermostatic load recovery [2].

Load voltage characteristics, or simply load characteristics, is an expression which gives the active or reactive power consumed by the load as a function of voltage and an independent variable called the load demand. Denoting load demand as *z*, the general form of load characteristics is as shown in expression 2.10

$$P = P(z, V)$$
$$Q = Q(z, V) \qquad 2.10$$

Exponential and ZIP (constant impedance, constant current, constant power) load models are some of the commonly used load models [2].

2.5 Generator Excitation Limits

Generators are the main source of reactive power in the power system. Their reactive capacity is limited by field current, armature current and end region heating limit or under excitation limit, as shown in Figure 2.6 [18]. This figure gives a tentative model of the reactive power capability of a generator. Power flow programs mostly model the generators as having reactive power limits as marked by the broken lines in Figure 2.6. This is a simple and conservative model of the capability curve. The maximum reactive power output is set using an over excitation limiter (OXL). Due to time-inverse characteristic of OXL, we have the generators cutting off reactive power supply after the

excitation current hits its limit. This can result in long term voltage instability. As soon as the OXL hits the limit, further increase in reactive power is not possible [20]. This is observed in PV and QV curves as a sharp discontinuity. In this thesis, the inability of Thévenin like methods to anticipate this discontinuity has been thoroughly explored.

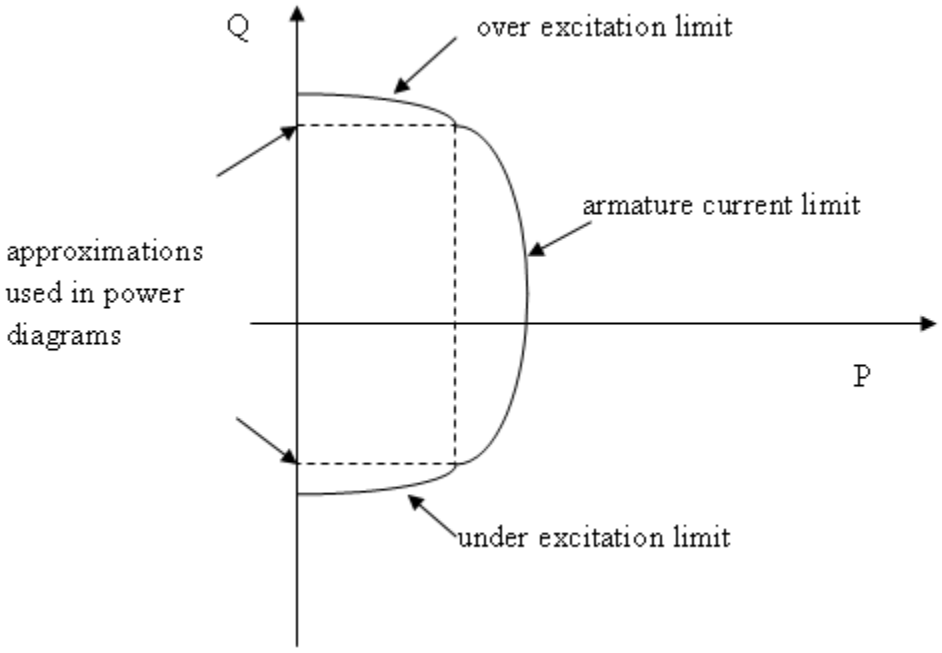

Figure 2.6 Generation capability curve

2.6 Types of Voltage Instabilities

Based on the severity and time of action of different devices there are four categories of voltage instabilities [1] have been quoted in the following paragraphs.

"Large-disturbance voltage stability *refers to the system's ability to maintain steady voltages following large disturbances such as system faults, loss of generation, or circuit contingencies. The study period of interest may extend from a few seconds to tens of minutes."*

***"Small-disturbance voltage stability** refers to the system's ability to maintain steady voltages when subjected to small perturbations such as incremental changes in system load. This form of stability is influenced by the characteristics of loads, continuous controls, and discrete controls at a given instant of time. This concept is useful in determining, at any instant, how the system voltages will respond to small system changes."*

***"Short-term voltage stability** involves dynamics of fast acting load components such as induction motors, electronically controlled loads, and HVDC converters. The study period of interest is in the order of several seconds, and analysis requires solution of appropriate system differential equations."*

***"Long-term voltage stability** involves slower acting equipment such as tap-changing transformers, thermostatically controlled loads, and generator current limiters. The study period of interest may extend to several or many minutes, and long-term simulations are required for analysis of system dynamic performance."*

2.7 Voltage Stability Dynamics Using Network and Load PV Curves

In this section, the process of voltage stability dynamics is explained using the aid of network and load PV curves [2]. This is illustrated in Figure 2.7.

An operating point of a power system is the intersection of load characteristics and network characteristics. As long as there is a point of intersection between the two curves, an operating point can be obtained. Consider a contingency that results in a new network PV curve and hence the system moves from point **a** to point **b**. Point **b** corresponds to the short term load characteristics. In the long term, the power restoring devices act on the system. This gives the final operating point **c'** through **c**. The vertical

line **ac'** is the long term load characteristics. The intersection implies that the system is able to restore power at steady state. In the steady state analysis, constant power characteristics of the load is assumed, which is also the most restrictive assumption.

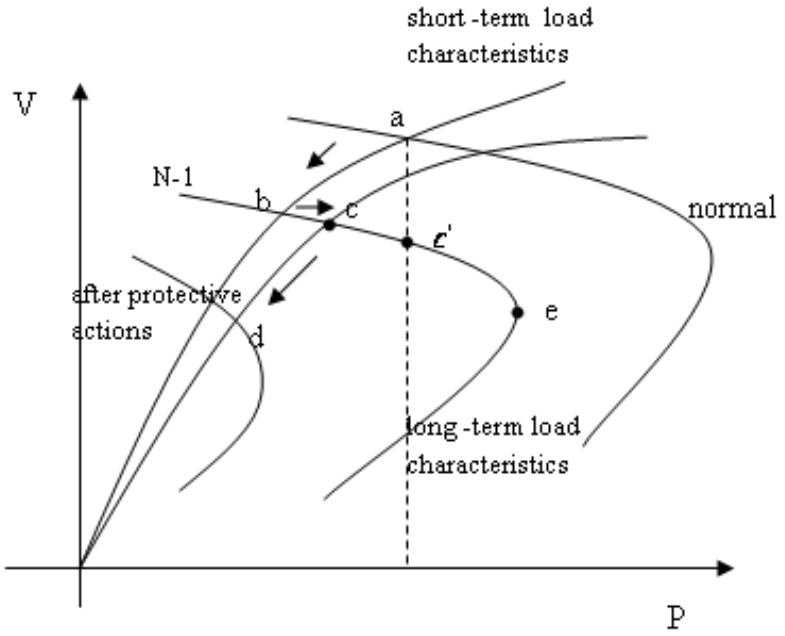

Figure 2.7 Voltage stability dynamics sequence

Consider the outage of another device from the system at point **c**. Consequently we have a smaller PV curve and the new point of intersection is **d**. However, there is no intersection between the load and network curves in the long run. The system then becomes long term voltage unstable.

2.8 Conclusion

This chapter gives a general overview of the mechanism of voltage instability tools available for study and factors to be taken into consideration for improving the voltage stability. For an extensive voltage stability assessment of a system, all of these factors have to be taken into account. The details in modeling should be included

intelligently. For example, it is not necessary to model the dynamics of the load restoration devices and fast acting loads if the purpose is to find the static stability margin of the system. Drawing the PV curve with constant power models is sufficient for that purpose. On the other hand to determine the control actions in order to overcome short term voltage instability the detailed modeling of load and timing sequence of different devices becomes necessary. For the online voltage stability monitoring to estimate the static voltage stability margin, it is customary to model loads as constant power and generators to have constant reactive power limits.

3 REVIEW OF ONLINE VOLTAGE SECURITY MONITORING

3.1 Overview

Power system security is the ability of the system to survive likely disturbances (contingencies) without interruption to customer service. Basic framework for security was first proposed by Dy Liacco [21]. He considers the power system as being operated under two sets of constraints: *load constraints and operating constraints.*

The load constraints impose the requirement that the load demands must be met by the system. The operating constraints impose maximum or minimum operating limits on system variables and are associated with both steady-state and dynamic stability limitations. The conditions of operation can then be categorized into three operating states: *normal, emergency and restorative.* The conceptual framework established by the three operating states has been illustrated in Figure 3.1. A system is in the *normal state* if both the load and operating constraints are met. A system is in the *emergency state* when the operating constraints are not completely satisfied. A system is in the *restorative state* when the load constraints are not completely satisfied. This is the case of either a partial or a total system shutdown.

This research is focused on the security monitoring aspect, where the objective is to determine if the power system is operating in normal state using the real-time measurements. The method developed can be extended to security analysis by considering a contingency list.

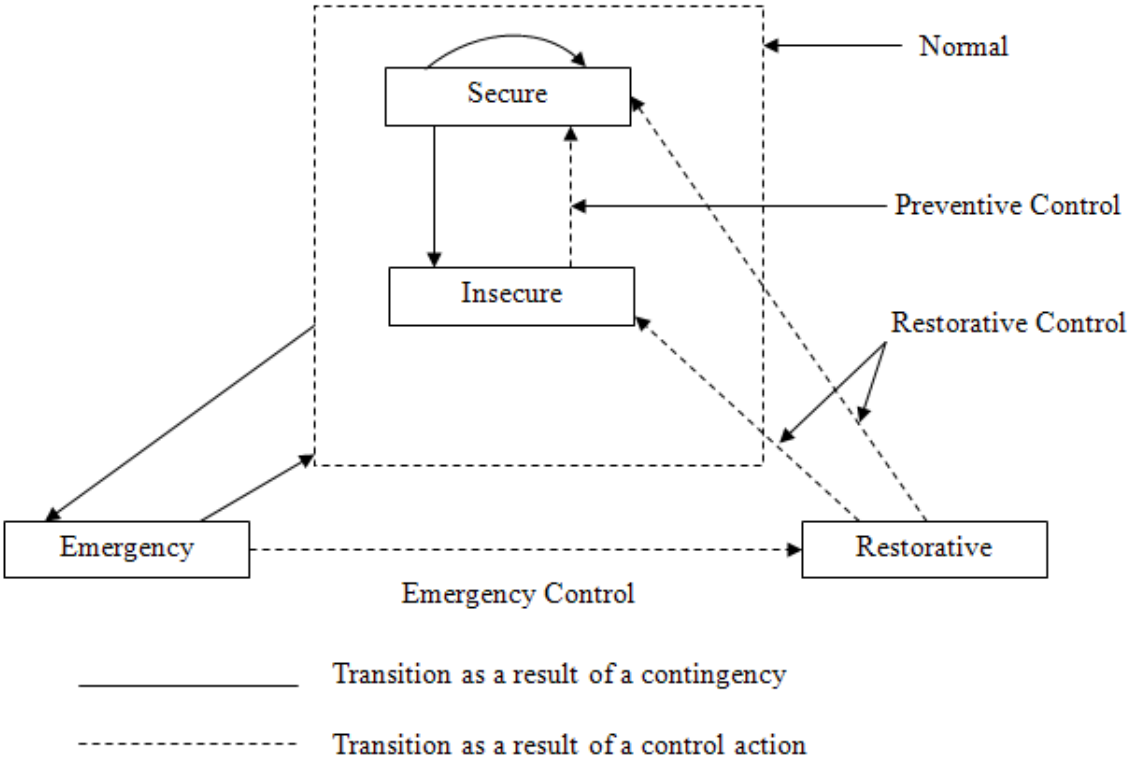

Figure 3.1 Power system operating states and the associated state transitions due to contingencies and control functions

Online security monitoring poses the problem of finding the distance of an operating point from stability. The measure obtained may be qualitative or quantitative. Qualitative measure doesn't give the exact megawatt (MW) margin but some number that can be interpreted in terms of stability, known as an index. Quantitatively we know exact MWs from distance to stability with respect to a credible scenario. Finding MWs can be computationally intensive, so the focus is in generating a voltage stability index. For online applications, these indices are such that they can be calculated from the available online measurements. This thesis however, proposes a fast method of accurately getting the quantitative measure of voltage instability from online measurements. Alternately, offline calculations and stored measurements can be used to build a statistical model of the power system. In the following sections, state of the art on index based voltage

instability measure and artificial intelligence based voltage instability measure are briefly discussed.

3.2 Index Based Voltage Instability Measure

There are certain irregularities or uniqueness in the system behavior towards the onset of voltage instability. The index based instability measure captures this unique system behavior in terms of a number and interprets them to give the notion of distance to instability. The indices can be used as a reference value to run a control routine. Some examples of system characteristic towards voltage instability are-the singularity of load flow Jacobian as discussed in Chapter 2, the generators hitting their reactive power limits, Thévenin equivalent approaching load impedance, etc.

3.2.1 Index from Direct Phasor Measurements

There has been a drive for getting voltage stability index directly from phasor measurements with the installment of Phasor Measurement Units (PMUs). The PMUs can give an accurate measure of voltage and current phasors in a snapshot. Phasor measurements have been applied for the calculation of voltage collapse proximity index in radial networks [22, 23]. The phasor measurement based approach for estimation of voltage stability index can be extended to general systems [3, 24, 25]. The method is fast, but yields poor accuracy.

In a study done by Haque [26], a prediction algorithm for the Thévenin equivalent is proposed. The proposed approach fails to address the issue correctly as the reactive power reserves of the system have not been taken into account during prediction of voltage stability margin. Begovic and Milosevic [27] use availability of reactive power

reserves without any discussion of the relationship with the Thévenin equivalent. The simplest version of Thévenin equivalent method can be described as follows [3]:

Figure 3.2 is a Thévenin equivalent representation of the power system with respect to the load bus under consideration. By equating the receiving and sending end currents we get the expression 3.1.

$$\frac{P+jQ}{\bar{V}} = \bar{I}^* = \left(\frac{\overline{\bar{E}_{th}} - \bar{V}}{Z_{th}}\right)^* \qquad 3.1$$

$$(P+jQ)Z_{th}^* = \bar{V}(\bar{E}_{th} - \bar{V})^*$$

Equation 3.1 is quadratic in $\bar{V}$ and there are two solutions for a given power demand: $P+jQ$. By symmetry, if $\bar{V}$ is one of the solutions then $(\bar{E}_{th} - \bar{V})^*$ is the other. The two solutions will be equal at the maximum power transfer and the solution will cease to exist for the demand beyond the maximum power transfer.

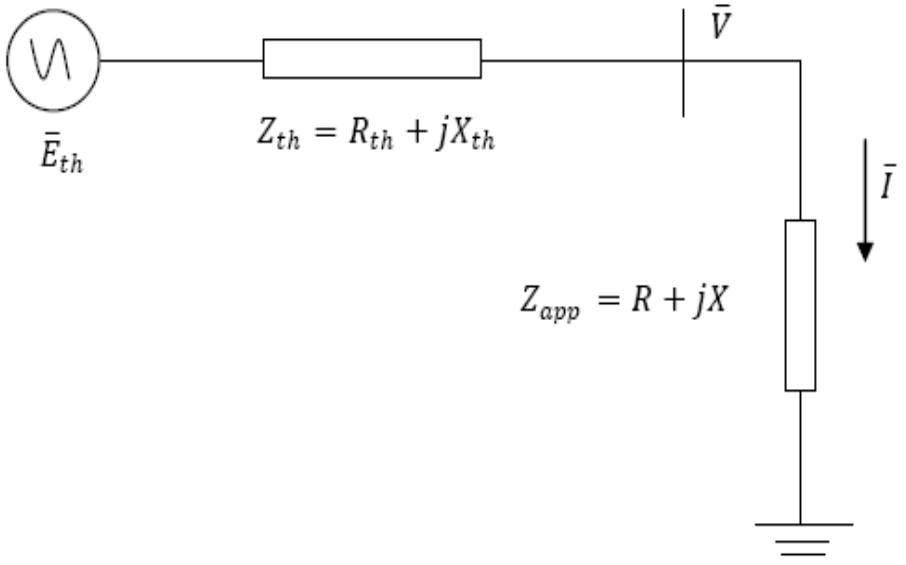

Figure 3.2 Thévenin equivalent representation of the power system

Hence, at maximum power transfer, relations 3.2, 3.3 and 3.4 exist.

$$\bar{V} = (\bar{E}_{th} - \bar{V})^* \qquad 3.2$$

$$or, \bar{Z}_{app} \times \bar{I} = (\bar{Z}_{th} \times \bar{I})^* \qquad 3.3$$

$$or, |\bar{Z}_{app}| = |\bar{Z}_{th}| \quad 3.4$$

The apparent impedance $\bar{Z}_{app}$is calculated as the ratio of voltage and current phasors measured at the bus. The distance between the parameters, $\bar{Z}_{app}$ and $\bar{Z}_{th}$ gives the margin for stability, which can be directly related to power margin.

To determine the *Thévenin Equivalent,* consider the equation 3.5.

$$\bar{E}_{th} = \bar{V} + \bar{Z}_{th}\bar{I} \quad 3.5$$

In equation 3.5, $\bar{V}$and $\bar{I}$ are measurable quantities. They are the measurements obtained from PMU. Since equation 3.5 has two unknowns- $\bar{E}_{th}$ and$\bar{Z}_{th}$, at least two measurements are required to estimate them. One of the drawbacks of the method that can be pointed out here is the required interval between the readings. The time window for measurement should be such that the loading condition changes but the network conditions do not. The assumption is reasonable but can't be guaranteed. Pal et al [24], propose a solution to this issue by proactive movement of the tap changer transformer. To avoid multiple readings for the Thévenin equivalent, Larsson et al [25] have limited the application to transmission line corridor. For the case of two readings, $\bar{E}_{th}$and $\bar{Z}_{th}$can be directly calculated as in equation 3.6 involving complex calculations.

$$\bar{E}_{th} = \frac{\bar{I}_1\bar{V}_2 - \bar{I}_2\bar{V}_1}{\bar{I}_1 - \bar{I}_2}$$
$$\bar{Z}_{th} = \frac{\bar{V}_2 - \bar{V}_1}{\bar{I}_1 - \bar{I}_2} \quad 3.6$$

For a general case, let $\bar{E}_{th} = E_r + j\bar{E}_i, \bar{V} = u + jw \; and \; \bar{I} = g + jh$. Thus equation 3.5 can be broken down into real and imaginary parts and written in the matrix form as in expression 3.7.

$$\begin{bmatrix} 1 & 0 & -g & h \\ 0 & 1 & -h & -g \end{bmatrix} \times \begin{bmatrix} E_r \\ E_i \\ R_{th} \\ X_{th} \end{bmatrix} = \begin{bmatrix} u \\ w \end{bmatrix} \quad 3.7$$

Decomposing 3.7 we get,

$$1.E_r + 0.E_i - g.R_{th} + h.X_{th} = u$$
$$0.E_r + 1.E_i - h.R_{th} - g.X_{th} = w \quad 3.8$$

Equation 3.8 is a multi linear equation. The coefficients which are the real and imaginary parts of Thévenin source voltage and impedance can be determined by the method of least squares [28].

3.2.2 Index from Load Flow Jacobian

The use of singularity of the power flow Jacobian matrix as an indicator of steady-state stability was first pointed out by Venikov et.al [29], where the sign of the determinant of the load flow Jacobian was used to determine the system stability. As discussed in Chapter 2, the singularity of load flow Jacobian doesn't necessarily mean that the system Jacobian is also singular. However, for voltage collapse and voltage instability analysis, any conclusions based on the singularity of the standard load-flow Jacobian would apply only to the phenomenon of voltage behavior near maximum power transfer [17]. Such analysis would not detect any voltage instabilities associated with synchronous machine characteristics or their controls. G_y approaches singularity as the system loading is gradually increased.

Based on these assumptions we have methods related to singular value decomposition, eigenvalue decomposition and test function techniques [4, 5, 30, 31]. The idea is to track the minimum singular value or eigenvalue of the system. The smaller the value, closer the system is to collapse. This information is embedded in the right and left

eigenvectors associated with the critical eigenvalue which will be discussed shortly. However, the smallest eigenvalue (or the singular value) may not be the most sensitive and some other eigenvalue may approach singularity even more quickly. Thus, it might be critical to track a number of eigenvalues. The methods give a very good insight about the system such as critical buses and critical stress directions with respect to voltage collapse.

The Gao et al [5] discuss the eigenvalue decomposition technique for voltage stability index determination. The decomposition may be applied directly to the reduced load flow Jacobian matrix as it is quasi-symmetric [31] and, therefore diagonalizable. Furthermore, due to quasi-symmetric structure, one expects to obtain a set of only real eigenvalues and eigenvectors, very similar to the corresponding singular values and singular vectors.

3.2.3 Other Techniques

L-index [32, 33] is another important voltage instability index whose feasible value ranges from 0 to 1. Values closer to 1 suggest that the system is closer to instability. The limit criterion is such that both load flow Jacobian singularity and the maximum power transfer theorem hold true.

Availability of reactive reserves has a direct relationship to the voltage stability margin. Voltage instability is a local problem as reactive power cannot be transported to long distances due to the inherent inductive nature of the transmission system. As a result many studies have explored the role of system reactive power sources such as synchronous machines, switched capacitors and static voltage controllers towards contribution in voltage stability. [6, 34, 35, 36, 37, 38, 39, 40, 41]

L.H. Fink [6] proposes real-time reactive security monitoring by monitoring the contingent VAR (voltage ampere reactive) margins of all the zones within a given system. Zones are a group of one or more “tightly” coupled generator buses, together with the union of the sets of load buses that they mutually support. The idea behind the method is that the voltage stability problem has a local origin and that it is directly related to the availability of reactive power sources. Schlueter [34-36] proposes the determination of proximity to voltage collapse by monitoring the reactive reserves. The reactive reserves are obtained by determining VCAs. In a recent method [37], VCA is determined directly by the method of sensitivity.

Further, in reactive reserve monitoring, use of switched capacitors to maintain VAR reserves in a system [38] and use of generator rotor heating level as an indicator of system voltage stability [39] have been suggested. BPA developed a system that monitored many key generators [40]. This work introduced an index that measured the total reserve level of a system. A small index value would mean that the system is short of VAR reserve. However, the method did not quantify the relationship between the VAR reserve level and the voltage stability level. As an extension, Bao et al [41] proposed a method to relate the VAR reserve level with voltage stability margin by monitoring certain key generators which have a prominent role in determining the level of voltage stability through their reactive reserves. This is a very good indication of use of reactive reserve for voltage stability margin determination.

3.3 Artificial Intelligence Techniques

Intelligence to the monitoring tools can be inputted via simulation (experimental data) or scientific rules or rules based on ad hoc knowledge of experienced operators. These techniques are called artificial intelligence techniques. For the tools to perform better we need to train them with as much data and scenarios as possible. It is up to us to decide how large a dataset we want to work on. This is important because it is possible to literally have infinite number and dimension of data points. Dimension meaning the number of variables under observation. Both number and dimension of data is important to reduce the training time, complexity as well as accuracy of the result.

An important classification of artificial intelligence techniques is based on their inductive or deductive nature. Inductive techniques gather information or develop a model from the available data directly to give the decisions while the deductive technique works on the set of rules and series of deduction before coming to a conclusion. The rules have to be fed via experts or these could very well have been generated from data itself. The deductive machines are also called expert systems. It is difficult to generate rules for deduction especially for very complex systems such as power systems which makes inductive techniques more attractive.

Some of the popular artificial intelligence approaches are expert systems, decision trees, artificial neural networks, genetic algorithms and fuzzy systems.

As mentioned, expert systems are deductive machines. Expert systems can be compared to human operators with much faster response. The speed is highly desirable because humans would have very little time to react against sudden and large disturbances which can cause the system to collapse in split seconds. An expert system package has four main parts: Inference Engine (IE), Knowledge Base (KB), Data Base (DB) and Explainer. The information from state estimation, security assessment and the

generator reactive reserves forms the DB. The IE takes the data in the database to interrogate rules in knowledge base. [9] L-index can be an input to the expert system. Based on the index values decision is made according to the predefined if-then rules. [10]

The artificial neural network (ANN) approach [14, 15], decision tree approach [11, 12, 13] , k-nearest neighbor approach [42] are inductive learners. The decision tree technique is a classification technique that can be used in voltage stability assessment to categorize a given operating state as either stable or unstable. However, we can also have a range of stability margin. One of the goals of the thesis is the study on improvement of decision tree approach as applied in voltage instability of power systems. The details will be provided in the fifth chapter. K-nearest neighbor technique is another simple classification method. This method is based on voting system. A new operating point is classified based on its proximity to the training instances. Let K=5. If a proximity measure gives 3 instances close to the test vector that are stable and 2 close to those that are not stable then the test vector is classified as stable.

ANNs have been used in voltage stability analysis to detect voltage instability (i.e. classification) and function approximation (estimating margin). The input to the model is power flow results and the output is an index such as L-index or index based on singular value decomposition (SVD). Just like the decision trees ANNs are trained off-line using previous data.

The genetic algorithms (GAs) [43] are used in voltage stability based problems for planning and other optimization situation. They are search algorithms which find the fittest combination of variables or the optimal set. They can be used to support decision trees or ANNs in reducing the attributes of the dataset. Fuzzy theory [44] is also used in aid with machine learning approaches. In voltage stability problems the magnitude of output variable is employed to label the voltage security levels.

3.4 Conclusion

In this chapter a broad picture of power system security assessment has been presented. It gives us the background to understand the relevance of the work involved in this thesis. Literature survey of the currently employed methods has been systematically presented. It has been emphasized that computational efficiency (speed) is the key element for online stability monitoring. The drive towards the goal has either been through increasing the power of computational devices (i.e., having parallel machines) or by reformulating the problem such that the information is interpreted differently requiring less computational effort (i.e. index). The later is the philosophy behind using the voltage instability indices.

Data from field measurements can be important source of system information. Using artificial intelligence techniques information from the data can be extracted for stability monitoring. This chapter also gives an introduction to those techniques and provides a foundation for the fifth chapter.

4 VOLTAGE STABILITY MARGIN PREDICTION USING REACTIVE POWER AVAILABILITY

4.1 Overview

.

The analysis of voltage stability phenomenon is performed statically or dynamically depending upon the requirement. The static method is used to estimate the voltage stability margin from the current operating point for a given scenario. PV curve tracing based on continuation power flow [16] is one such tool. Index from load flow Jacobian is useful for static voltage stability monitoring. On the other hand dynamic voltage stability analysis is to understand the voltage stability mechanism and determine the control actions such as maintaining reactive power reserves, generator excitation limiter actions, capacitor switching, transformer tap setting and others through time domain simulations [45, 46, 47]. These methods are computationally burdensome; therefore their adoption in the real-time environment is infeasible.

With the development of PMUs and wide area measurement system, high level accuracy and speed is achieved in measurement of the power system states. Sufficient number of PMU location gives complete state estimation of the system [48, 49]. Various efforts [3, 22-27, 50, 51] have been made in order to apply the fast and accurate phasor measurements for real time voltage stability monitoring. Artificial intelligence methods as discussed in Chapter 3 use the phasor measurements to assess the current system conditions and give the voltage stability information based upon model developed from the stored measurements. Alternately we have methods based on local phasor measurements that can be implemented in a distributed manner so as to account for the entire network. The proposed methods as mentioned are heavily dependent on the accurate estimation of the Thévenin equivalent. Gubina et al [50] and Corsi [51] have

proposed more accurate methods of Thévenin equivalent estimation. The method however has one further issue of not being able to adjust for the effect of the generators hitting their limits. The forecast is exact if the network equivalent stays unchanged and if no limiting devices act. The forecast is believed to be optimistic but no further discussion on the resolution of the issue is available. [52] Because of the discontinuous change in Thévenin equivalent (when a generator hits the limit) it is not recommendable to directly predict Thévenin equivalent or its direct derivatives. Other voltage stability indices [4, 5, 30-33] also share this characteristic of having discontinuity when the generators hit their limits. Thus, it is essential to take into account the reactive supply depletion when predicting an index or a margin. The work here identifies a systematic approach to take care of the discontinuous drop of network strength due to exhaustion of reactive power supply to a bus. The real time observations that we need are reactive power generation of different generators and the loading at the different buses. This data is readily available from the SCADA. Given the observability of the system via PMUs, direct phasor measurements could be used for the margin prediction.

In section 4.2 background and the motivation of the method is presented. The application of the method for various scenarios has been proposed in section 4.3. Section 4.4 describes the online implementation of the method. The results are demonstrated in section 4.5. Finally section 4.6 gives the concluding remarks.

4.2 Background and Motivation

The objective here is to predict the maximum loadability of a bus (point 'B', Figure 4.1) from a given operating condition (point 'A' Figure 4.1). In this work, using the real time measurements, the task has been accomplished by a blend of offline and on line calculations.

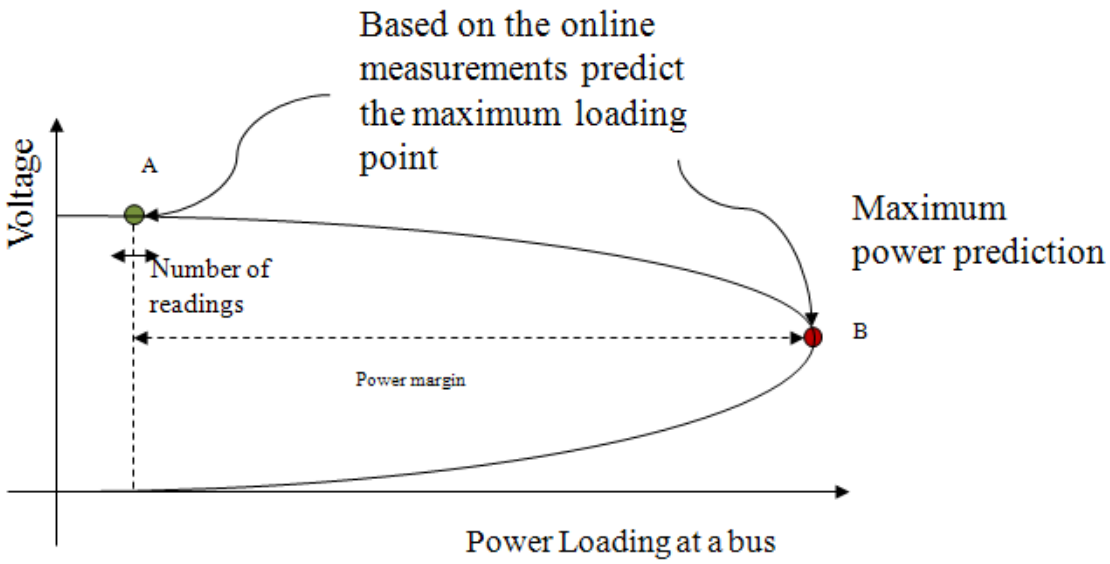

Figure 4.1 Reactive power and margin estimation

The over prediction of stability margin due to Thevenin equivalent is because the prediction is in terms of network strength. However, power systems are more often choked off of reactive supply. As a result we have a voltage instability situation much before the limit obtained using the maximum power transfer theorem (the case for Thévenin and similar methods). Schlueter [36] discussed manifestation of voltage instabilities. The exhaustion of reactive power sources for a given voltage control area (VCA) or loss of voltage control is followed by exponential increase in reactive power loss (clogging). Clogging can completely choke off the reactive power flow to the VCA needing reactive support.

The Thévenin equivalent method draws our attention to the type of voltage instability where the network is no longer able to transfer power. This is a case that would arise with sufficient reactive power but insufficient network strength.

Hence, considering the two situations, ideally the power margin should be:

minimum (power margin by network, power margin by reactive power availability)

The two margins have been distinguished by classifying the buses as ‘reactive reserve limited’ and ‘transmission limited’ as an explanation to justify misclassification of some of the buses by the sensitivity based method [37]. The difference in margin due to shortage of reactive power and network strength can easily be demonstrated using a 3 bus system as shown in Figure 4.2. Buses 1 and 2 are strongly tied while the tie between buses 2 and 3 is relatively weak. Generator 1 is the primary source of reactive power for load at bus 2 while the generator at bus 3 is not.

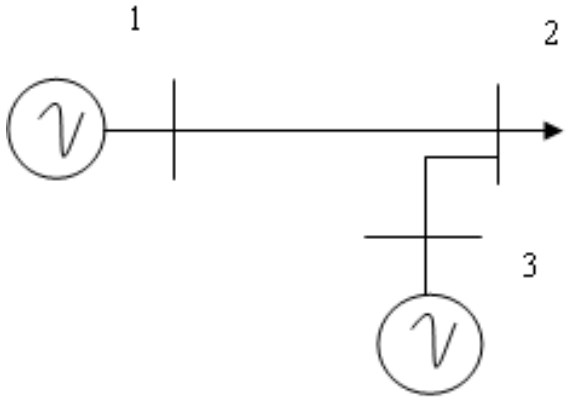

Figure 4.2 Three Bus Test System

Figure 4.3 is a plot of loading at bus 2 in the horizontal axis against the power predicted by Thévenin equivalent method in the vertical axis. The initial prediction (initial portion of the curve), approximately at 23 p.u. is the maximum power that could be transferred, if we had unlimited reactive supply. There is a sudden dip in predicted power margin at a loading of 6.7 p.u. At this point Generator 1 (reactive power limited at 4 p.u.) hits the limit and the power predicted drops to 8.0 p.u. Eventually, the power flow diverges at 7.9 p.u. It is the indication of generator at bus 3 hitting the limit as well. The

simulation of Figure 4.3 was done using various levels of reactive capacity (in Figure 4.3 the limit placed was 5 p.u.) of generator at bus 3 and fixed reactive capacity of generator at bus 1. Even after considerable increase in reactive capacity of generator 3 it was found that the increase in margin was not significant. Figure 4.4 is the corresponding PV diagram. The proximity of margin due to loss of voltage control (exhaustion of local reactive sources) and clogging is demonstrated [36].

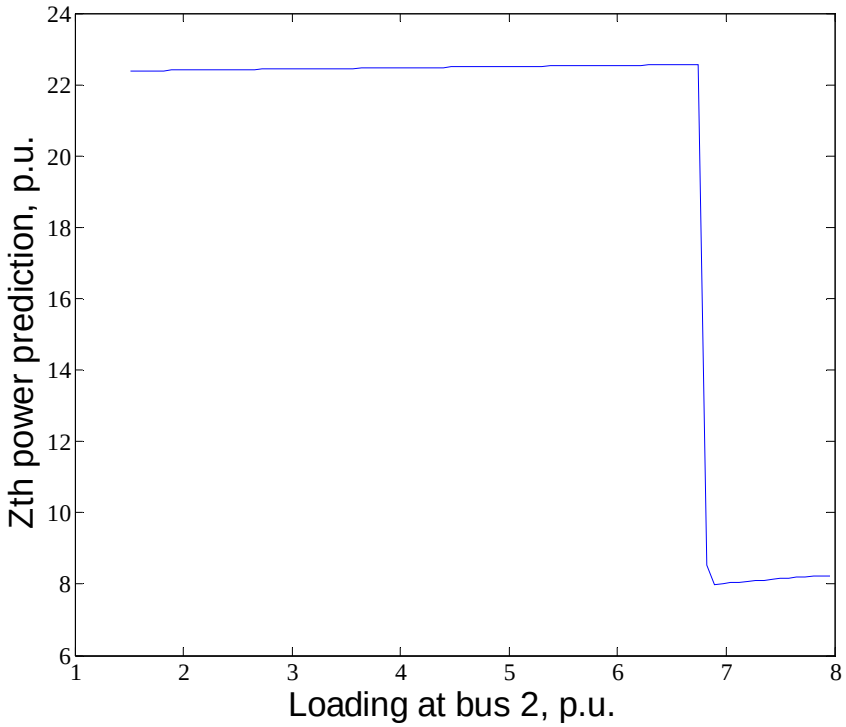

Figure 4.3 Thévenin power predictions with high limits on generator at bus 3

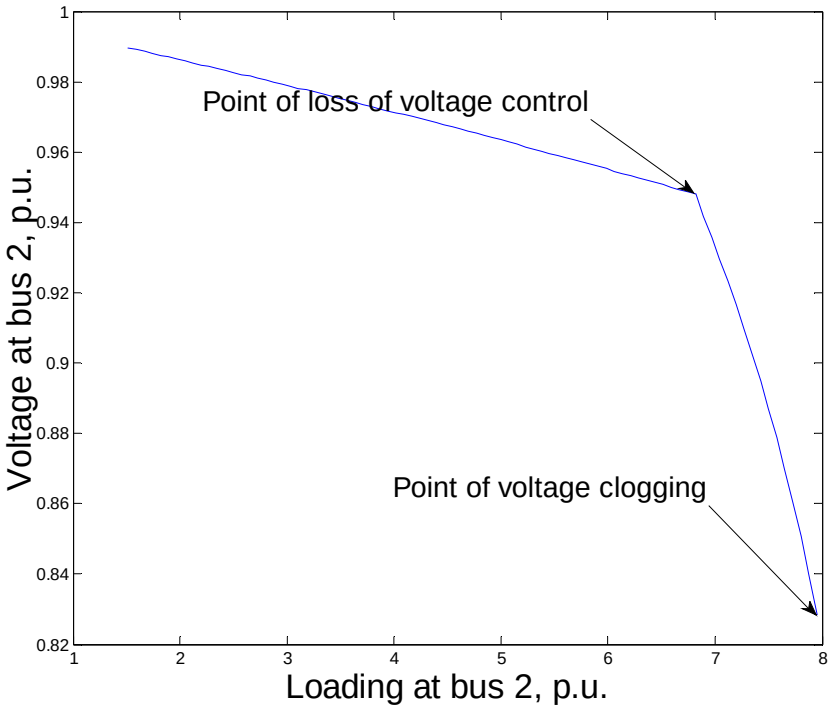

Figure 4.4 Maximum power obtained for reactive power limited generators

There are two observations:

- The maximum margin for loading at bus is influenced by reactive power availability at certain generators (here, it is generator 1 that influences the loading at bus 2)
- If we had the reactive reserves large enough then the maximum power transferable is constrained by the network limit (here 23 p.u. as predicted by the Thévenin model initially where the generator 1 hitting its limit was not anticipated). This situation wasn't observed for the test systems considered.

With the above observations it is therefore sufficient to consider reactive reserves contributing to point of loss of voltage control for the voltage stability margin prediction.

4.3 Proposed Method

Suppose, the maximum reactive power ($Q_{loadend}$) that can be supplied to a load bus is known. With the assumption that the load increases with constant power factor, the maximum real power ($P_{loadend}$) that can be transferred to a bus is given by equation 4.1.

$$P_{loadend} = Q_{loadend} \times cot\emptyset \quad (4.1)$$

Given the nonlinear nature of power system it is very difficult to estimate $Q_{loadend}$. The general form of reactive power equation for the maximum loading of a particular bus can be formulated as in equation 4.2.

$$Q_{total} = Q_{lossend} + Q_{networkend} + Q_{loadend} \quad (4.2)$$

Where,

Q_{total} : total reactive power that is consumed by the system at maximum loading of the given bus

$Q_{lossend}$: reactive power loss at maximum loading

$Q_{networkend}$: reactive power consumed by the rest of the network buses which may be a constant or may vary depending upon system scenario

$Q_{loadend}$: maximum reactive power loading of the bus under consideration

In equation 4.2, $Q_{loadend}$ can be determined only if Q_{total}, $Q_{lossend}$ and $Q_{networkend}$ can be estimated beforehand. Depending upon system complexity and scenarios different techniques need to be employed. Figure 4.1 gives a high level perspective of the margin estimation process. The flowchart in Figure 4.5 gives the outline of steps in power system operation environment which is self explanatory.

In the section that follows, step by step process has been developed for different scenarios and complexities of power system. First the method is explained for a simple two bus system and further elaborated on a multiple bus system to generalize the whole idea.

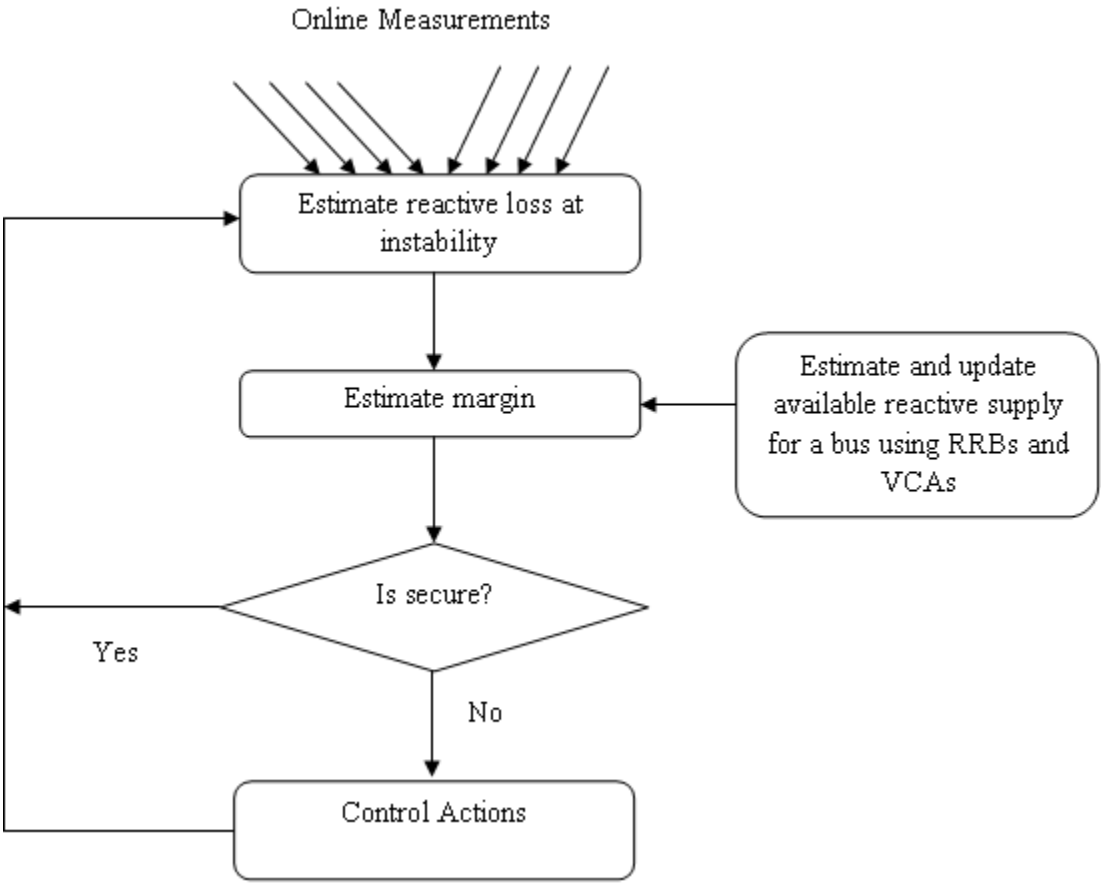

Figure 4.5 Flow chart of system operation with algorithm implementation

4.3.1 Two Bus System

For the two bus case, equation 4.2 reduces to 4.3 without the $Q_{networkend}$term.

$$Q_{total} = Q_{lossend} + Q_{loadend} \tag{4.3}$$

This is the simplest case possible as there is no interaction between different buses. The load and source are well defined. Q_{total} is the maximum reactive capacity of the generator . $Q_{lossend}$ is predicted using the observations of reactive loss and reactive power generation level. This is discussed in section 4.3.3.

4.3.2 Multiple Bus System

In this case the reactive power equation is same as equation 4.2. That is,

$$Q_{total} = Q_{lossend} + Q_{networkend} + Q_{loadend} \tag{4.4}$$

There are three quantities to be estimated before the value of $Q_{loadend}$ can be determined.

Q_{total} is the summation of maximum reactive powers of generators in the system (with the assumption that reactive power sources and sinks are strongly coupled). This implies, at the loadability limit all the generators will lose their voltage controllability.

$Q_{networkend}$ can be thought of as two types. One is the case where there is load increment in single bus while the other is the case where there are multiple load increments. For the first case $Q_{networkend}$is a constant and can be obtained by summing the reactive load demand at every other bus. For the second case a little modification in equation 4.4 is required. Considering proportional increase of load at all buses, the equation can be developed as follows. If, $Q_{network}$is the current network reactive power

absorption, Q_{load} is the current reactive power absorption by the given bus and Q_{avail} is the net total reactive power that is available for different loads excluding the losses, equation 4.4 for this system changes to equation 4.5.

$$Q_{total} = Q_{lossend} + Q_{avail} \tag{4.5}$$

By proportionality,

$$(Q_{load}/(Q_{network} + Q_{load})) \times Q_{avail} = Q_{loadend}$$

$$or, Q_{avail} = Q_{loadend}\left(\frac{Q_{load}}{Q_{network} + Q_{load}}\right)^{-1} \tag{4.6}$$

Replacing 4.6 in 4.5 we get,

$$Q_{total} = Q_{lossend} + Q_{loadend}\left(\frac{Q_{load}}{Q_{network} + Q_{load}}\right)^{-1} \tag{4.7}$$

Next $Q_{lossend}$ is to be estimated to determine $Q_{loadend}$ in equations 4.3, 4.4 and 4.7.

4.3.3 Determination of Reactive Power Loss

Figure 4.6 is a combined plot of reactive loss (Q_{loss}), predicted maximum reactive power loss (Predicted $Q_{lossend}$) and the Thevenin equivalent (Z_{th}) for a bus, versus the total reactive power generation of the system. The reactive power loss and Thevenin equivalent have been normalized by their corresponding largest value, while the predicted maximum reactive power loss has been divided by the actual maximum value of the reactive power loss. In Figure 4.6, reactive power loss is quadratic (approximately) while

the Thevenin equivalent impedance is discontinuous at the operating points where the generators hit their limits. Due to the smooth nature of the reactive power loss curve, it can be more accurately estimated compared to Thevenin equivalent. Given the quadratic nature, the reactive power loss has been modeled as a quadratic function of total reactive power generation in this study.

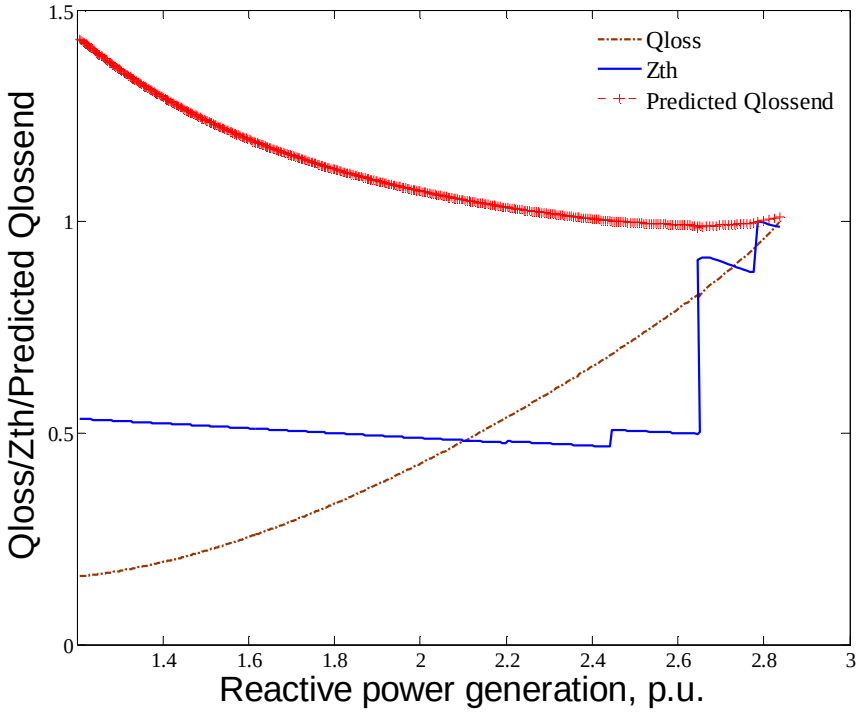

Figure 4.6 Combined plots of normalized $\boldsymbol{Q_{loss}}$, $\boldsymbol{Q_{lossend}}$ and $\boldsymbol{Z_{th}}$ with respect to reactive power generation for a typical system (here IEEE 30 bus system)

The quadratic modeling of the loss curve is given by equation 4.8.

$$Q_{loss} = aQ_g^2 + bQ_g + c \tag{4.8}$$

To determine the coefficients a, b, c at least three observations are needed. The method employed is the weighted least square estimation [53]. The weighted least square formulation is given by equation 4.9.

$$\begin{bmatrix} a \\ b \\ c \end{bmatrix} = (X \times W \times X')(X \times W \times Y) \qquad 4.9$$

Where,

$$X = \begin{bmatrix} 1 & 1 & 1 \\ Q_{g1} & Q_{g2} & Q_{g3} \\ Q_{g1}^2 & Q_{g2}^2 & Q_{g3}^2 \end{bmatrix} \qquad W = \begin{bmatrix} W^3 & 0 & 0 \\ 0 & W^2 & 0 \\ 0 & 0 & W^1 \end{bmatrix} \qquad Y = \begin{bmatrix} Q_{loss1} \\ Q_{loss2} \\ Q_{loss3} \end{bmatrix}$$

In order to get $Q_{lossend}$, Q_g in equation 4.8 is to be replaced by total reactive power available for the bus under consideration. This is Q_{total}- the reactive power generation at the instability limit. The weighing parameter 'W' gives more weight to recent observations. Formulation in 4.9 is for 3 sets of readings only.

Determination of reactive loss is one of the key steps in determining the voltage stability margin. There are two steps in determination of the $Q_{lossend}$ - *the estimation of coefficients* and the *total reactive power allocation* for a given bus. These elements determine the accuracy of the reactive loss, which eventually determines accuracy of the final prediction.

Figures 4.7 and 4.8 show the reactive power loss curves estimated at different load levels for the IEEE 2 and 5 bus systems. The plot is drawn with reactive power loss in the vertical axis and reactive power generation of the system in the horizontal axis. It shows how the loss curves vary with the obtained values of coefficients at different loading stages. The legends, 'coefficients1', 'coefficients2', etc correspond to the coefficients estimated at the initial part of the curve while the legend 'exact' is for the exact curve. The observed accuracy of coefficient estimation thus justifies the use of the method of weighted least square curve fitting.

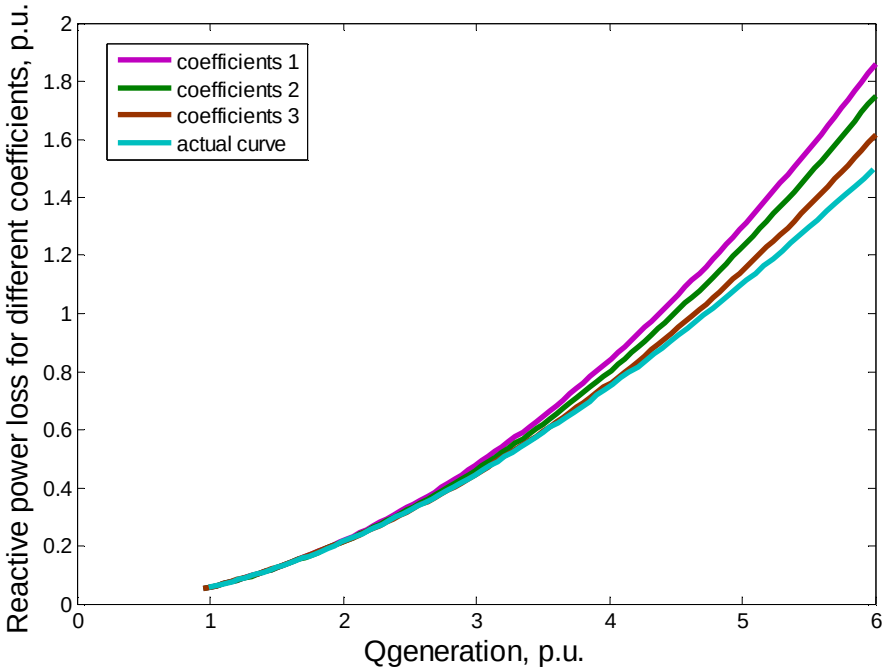

Figure 4.7 Variations of loss curves due to estimation error for 2 bus system

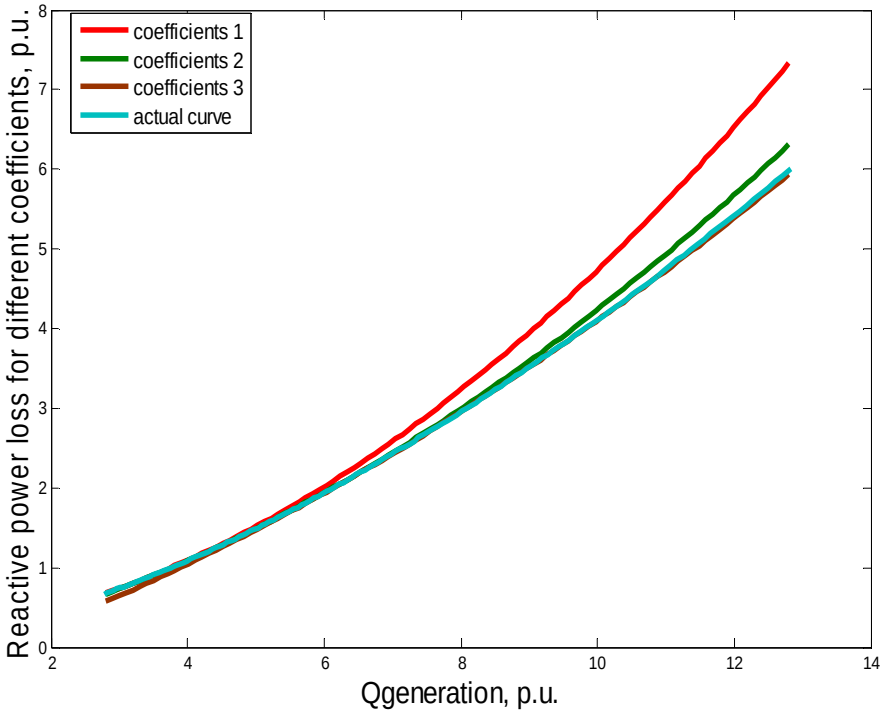

Figure 4.8 Variations of loss curves due to estimation error for IEEE 5 bus system

4.3.4 Issues

The issues involved in estimation of power margin are the determination of $Q_{lossend}$ and the estimation of reactive power allocation for a bus which also affects the $Q_{lossend}$ prediction. The reactive allocation problem is difficult for large systems with multiple VCAs. The procedure for large systems is explained in the following sections.

4.3.4.1 Application of the Method on Large Systems

For large systems, the coupling between buses varies. This gives rise to groups of coherent buses with varying sets of generators as a source of reactive power. Such groups are referred as VCAs [30]. It means that a bus cannot get its reactive power supply from every generator in the system (the reason why voltage problem is called a local problem). The equation 4.5 will not hold if we are to define Q_{total} as the sum of the reactive power capacity of all the generators. In order to determine which particular generators supply reactive power to which particular buses and in what amount (for generators supplying multiple buses), a feasible way of doing it is via the determination of VCAs. The set of generators exhausted at the minima of the QV curve of a bus *k* is the reactive reserve basin (RRB) for that particular bus and the set of buses with common reactive reserve basin comprise the VCA [30].

Considering the above definition, generators get associated with multiple VCAs. It is again inaccurate to consider the entire capacity of reactive reserve basins as the total reactive power supply for a VCA. For the scenario where the load is changing in all the buses of the system; it becomes very naïve to not acknowledge the fact that the reactive reserve basin for a given VCA would have a smaller capacity. Reactive reserve basin for a VCA would depend on participation of generators in that VCA defined here as

participation factors (PFs). A simple way to define the relationship is to consider proportionality. The error associated with this is that load sensitivities could be different i.e. every VCA may not have same sensitivity towards the generators to be generalized as a proportional relationship.

4.3.4.2 Algorithm to Determine VCA [36] and Participation Factors

There are various methods for determining VCAs [36], [37], [54]. For convenience and accuracy, the VCA is determined using QV curves [36]. Following are the steps for VCA and participation factor determination.

- Draw QV curve for each load bus.
- Determine the minima of the QV curve.
- The generators that exhaust for the minima are the participants in the RRB for that particular bus.
- Once generators have been determined for all the buses and buses with common reactive reserve basins sorted out; all the VCAs are determined.
- For a generator participating in 'n' VCAs, the participation factor of that generator in the RRB has been defined as follows:

  Participation Factor (*p.f.*) of the generator in VCA 'j'=

$$\frac{Q_j}{\sum_{i=1}^{n} Q_i} \tag{4.10}$$

  Hence the total reactive capacity of a VCA for *m* generator reactive reserve basin is:

$$\sum_{j=1}^{m} p.f_j \times Q_{maxj} \tag{4.11}$$

Where,

Q_j : total reactive power of a VCA

Q_i: total reactive power of individual VCAs

Q_{maxj}: maximum Reactive power capacity of a generator

$p.f_j$: participation factor of the generators

4.3.4.3 Applying Voltage Control Area

To know the amount of increment of load possible in a given bus for a multiple VCA system; the information from VCA is critical. Given the VCA we can simply take the reactive reserve basin as the total reactive source and perform prediction in that VCA. In effect the system has been reduced to a unit of closely coupled system with respect to reactive power exchange. The result is conservative because the bus under consideration could be sensitive to other generators which are not a part of the reactive reserve basin.

For a system with multiple load increase the participation factors become very useful. The generators are a part of more than one VCA with different sensitivities. Consequently, the exact amount of reactive power absorbed by a load bus cannot be quantified. The approximation is done by proportionality as in equation 4.11. Once this is done, the problem reduces to single VCA multiple load change. With this reduction, steps in section 4.3.2 and 4.3.3 can be undertaken for final margin estimation for the given bus.

4.4 Online Implementation of the Method

Schlueter [36] has indicated that VCAs are fixed. They do not change even when severe contingencies and operating changes occur. It is however apparent that line outages should change the VCA. The idea was tested on the IEEE 30 bus system by calculating

VCA following a contingency. It was found that the VCAs did change with respect to most contingencies. However, buses 25, 26, 27, 29 and 30 were part of the same VCA and the reactive reserve allocation to them did not change a lot. The plot for bus 26 of reactive power allocation with respect to contingencies is shown in Figure 4.9. The reactive reserve allocation is almost constant throughout the process which implies that VCAs are quite robust. The argument made by Schlueter [36] and the obtained result can be explained as follows:

It is not entirely correct that VCAs do not change with contingencies. However reactive power transfer is a local problem and the contingencies will influence only the local buses. Consequently, for every contingency there is no need to trace QV curve for all the buses. Only the buses closely affected by the contingency can be considered. One simple way would be to check the sensitivities of generator reactive power to the line that was out. The reactive reserve basin then needs to be calculated for only those buses which lie in the VCAs associated with the generator. This will drastically reduce the number of buses for VCA determination and make the process compatible to online implementation. Sensitivity based method [37] would further accelerate the process. Further investigation is needed to find out the exact computational advantage. For the IEEE 30 bus system result, the system is small; therefore most of the contingencies affect the reactive power flow. The buses mentioned (25, 26, 27, 29, 30) have similar reactive reserve capacity because these buses are relatively electrically isolated from rest of the system. The variation of reactive power observed in Figure 4.9 is for the contingencies related to transformer outages and a few major lines, otherwise the VCA essentially remains the same.

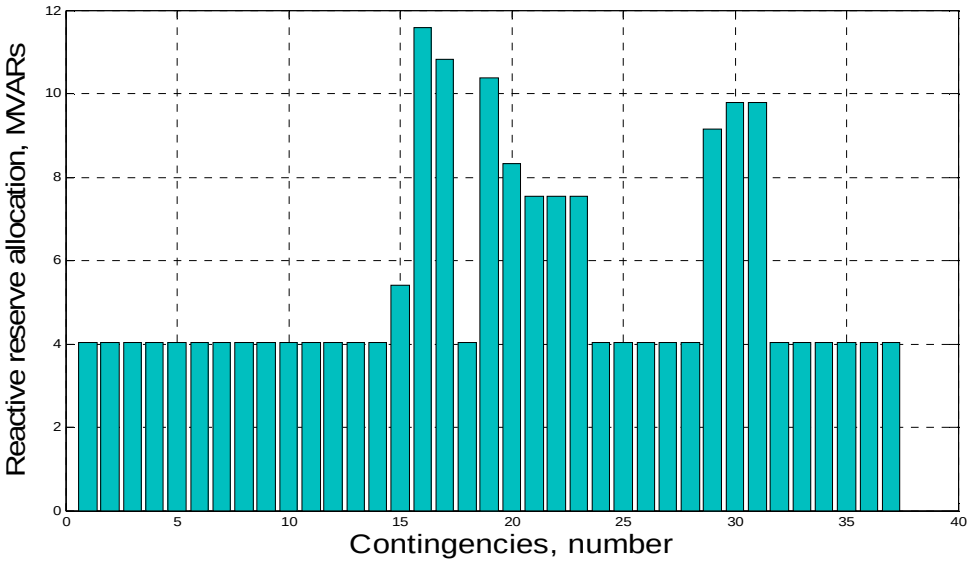

Figure 4.9 Reactive reserve allocations for bus 26 vs. contingencies

4.5 Results and Analysis

The method was applied to two bus system to understand the effectiveness. Further, simulations were done on IEEE 5 and 9 bus systems to cover all the scenarios mentioned. The IEEE 9 bus system is an example of a large system as it has multiple VCAs. Finally the result for the IEEE 30 and IEEE 118 bus system has been presented. In all cases, error was calculated using equation 4.12.

$$Error(\%) = \frac{P_{realmax} - P_{predictmax}}{P_{realmax}} \times 100 \qquad 4.12$$

Simulation was done by customizing routines in Matpower package [55]. The power system data also corresponds to the data file available in the Matpower package. The steps in simulations can be explained as follows. Given a bus, at least three observations were taken by varying the load (single increase or multiple increases). Using these values to estimate the coefficients of the quadratic equation $Q_{lossend}$ was predicted. The reactive reserve for each bus was calculated from offline simulations. Finally,

maximum power for a given scenario was predicted using the above formulation. For every error plot the horizontal axis represents the loading increase at a particular bus in p.u. and the vertical axis represents the prediction error at the corresponding operating condition for the same bus.

Figure 4.10 is the error plot for the two bus system using Thévenin equivalent method. Figure 4.11 is the error plot using the proposed method. The error in prediction due to Thévenin equivalent method is -156% as opposed to maximum error of 6.5% given by the proposed method for the same system. The negative sign denotes, over prediction of the maximum loading point.

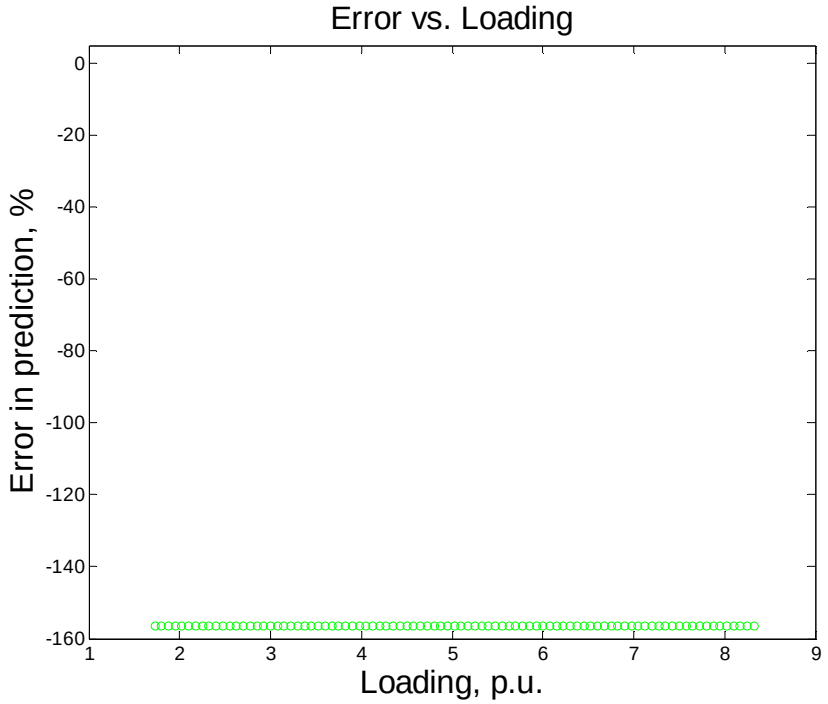

Figure 4.10 Error for the two bus system using Thévenin Equivalent method

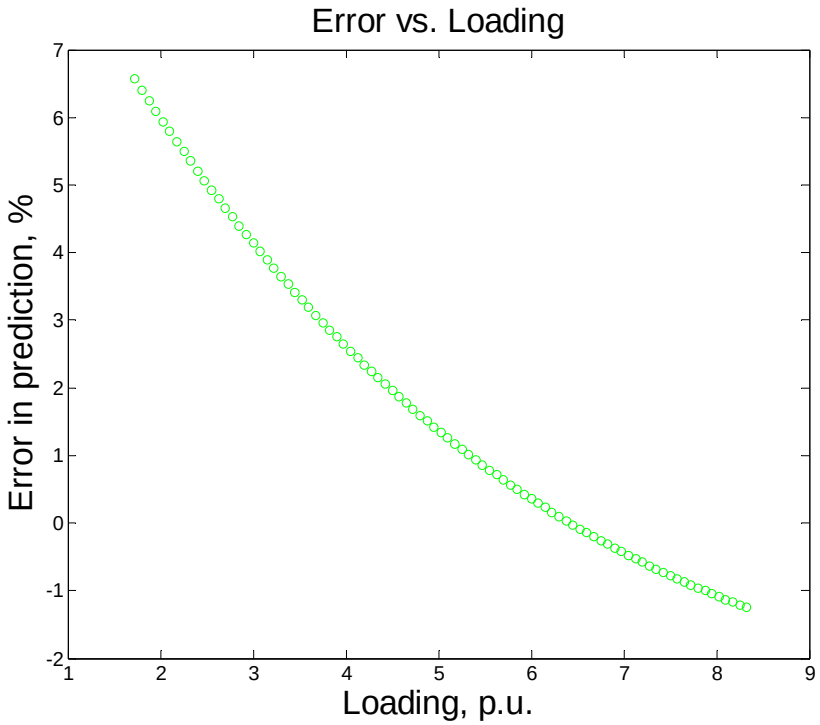

Figure 4.11 Error for the two bus system using the proposed method

The sources of error are the inaccuracies of Q_{total} and $Q_{lossend}$. Since this is a small system (two buses) $Q_{total}$is the maximum reactive capacity of generator. The error seen is thus due to error in prediction of reactive power loss. The initial error can be attributed to the fact that we have very few measurements to work with. Once we have sufficient number of points, the prediction of $Q_{lossend}$ becomes accurate. The IEEE 5 and 9 bus systems have multiple buses with multiple loads, hence there is a flexibility to predict with single and multiple load changes. In both the cases the accuracies due to the new method is very good (Table 4.2).

Figure 4.12 is the one line diagram of IEEE 30 bus system. It has 6 generators, 42 lines, a base load of 272.4 MW and 107.80 MVAR and a maximum loading of 490 MWs. The VCAs have been outlined in Figure 4.12 and presented in Table 4.1 with corresponding reactive reserve basins and participation factors. The results are much more accurate than predicted by Thévenin like methods. Bus 3 has been chosen for

observation. Error plots can be seen in Figures 4.13 and 4.14. Next, as a test of the method for a larger system IEEE 118 bus system was used. There are 186 branches, 54 generators with 29 VCAs and the base load observed was 4242 MW and 1438 MVAR with final loading of 6363 MWs. The prediction was done for bus 21 and the error plots can be observed in Figures 4.15 and 4.16 respectively for the two scenarios.

Table 4.1 VCAs and RRBs with PFs for IEEE 30 bus system

VCA_ID	**Buses in VCA**	**RRBs (Generators)**	**PFs**
1	3,4,6,9,10,12,28	1,2,5,8,11,13	0.53,0.28,0.53,0.19,0.42,0.21
2	7	1,2,5,8,13	0.47,0.24,0.47,0.17,0.18
3	14,18,19,20,23,24	8,13	0.23,0.25
4	15,16	2,8,13	0.10,0.07,0.07
5	17,21,22	2,8,11,13	0.38,0.27,0.58,0.29
6	25,26,27,29,30	8	0.07

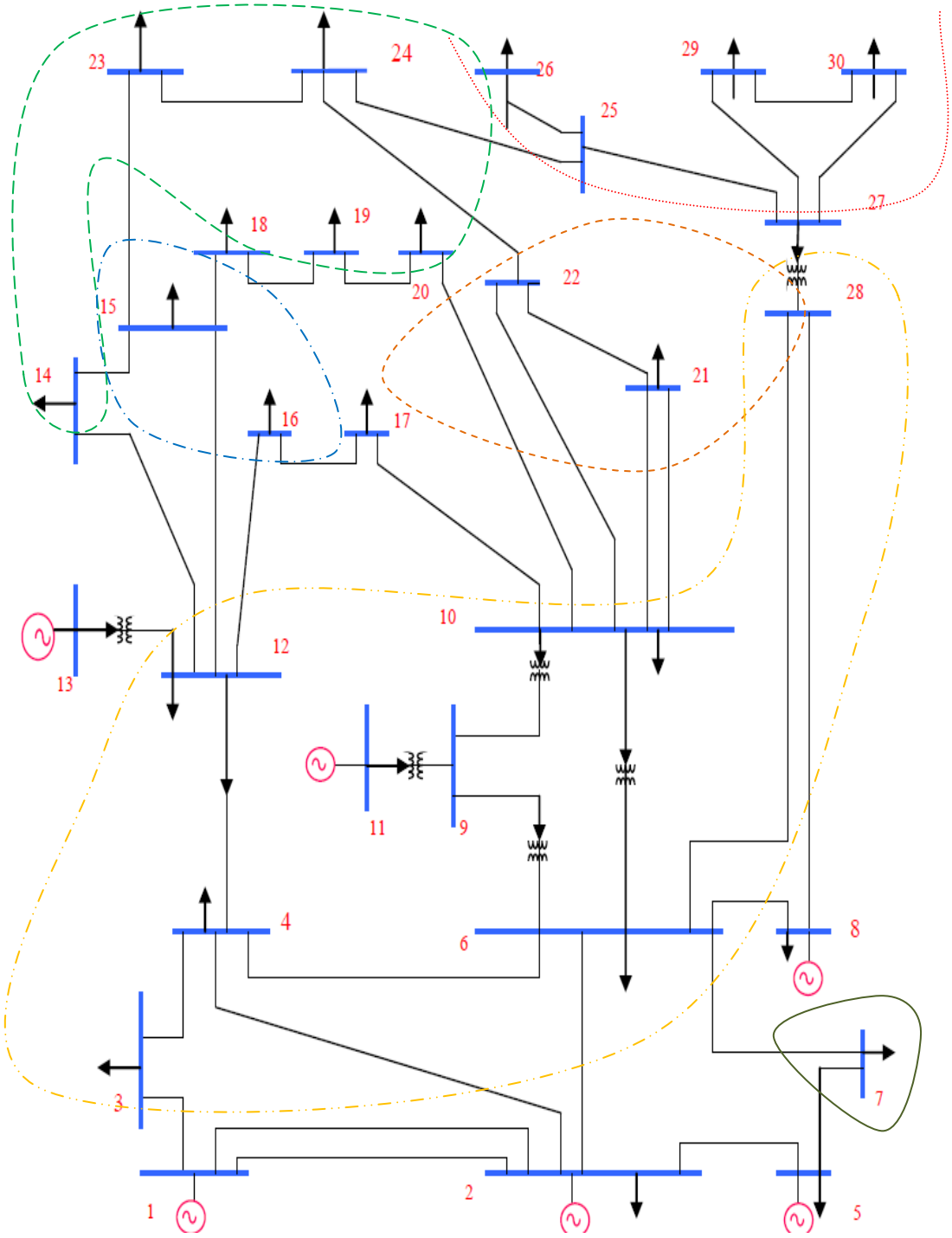

Figure 4.12 IEEE 30 bus system

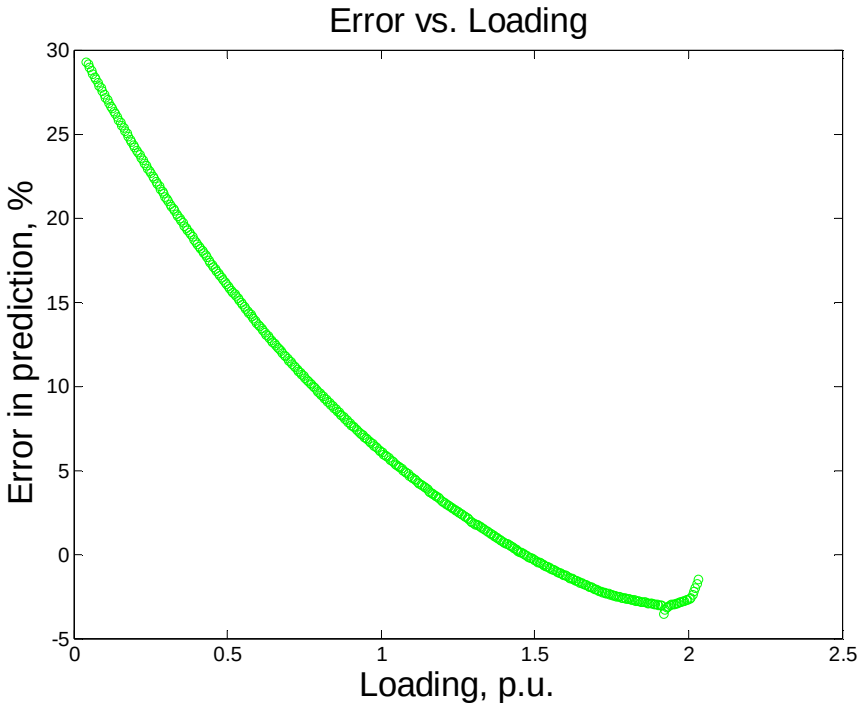

Figure 4.13 Error for IEEE 30 bus system at bus 3, single bus load increase

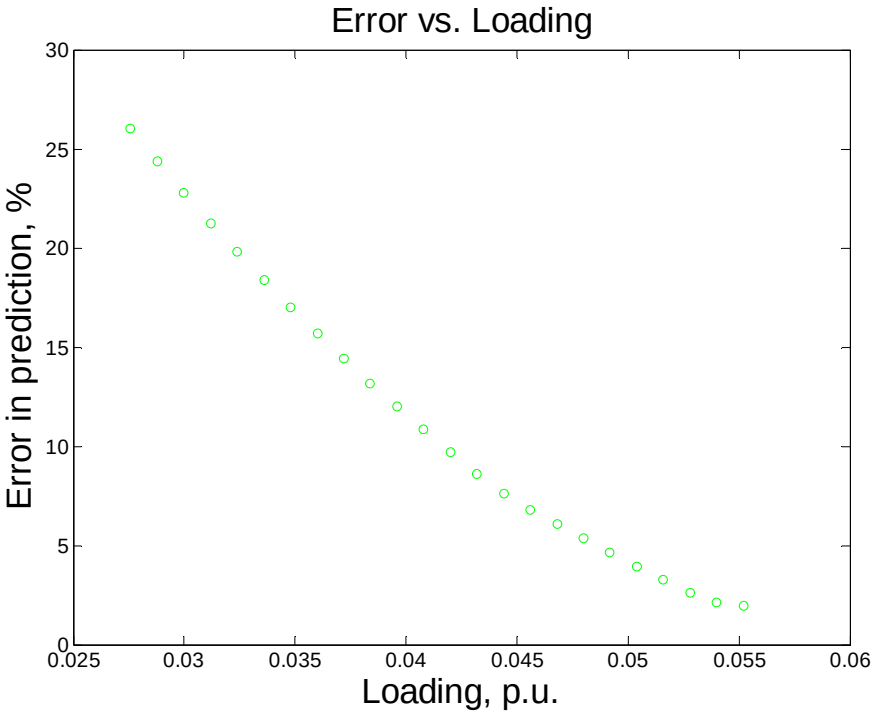

Figure 4.14 Error for IEEE 30 bus system at bus 3, multiple load increase

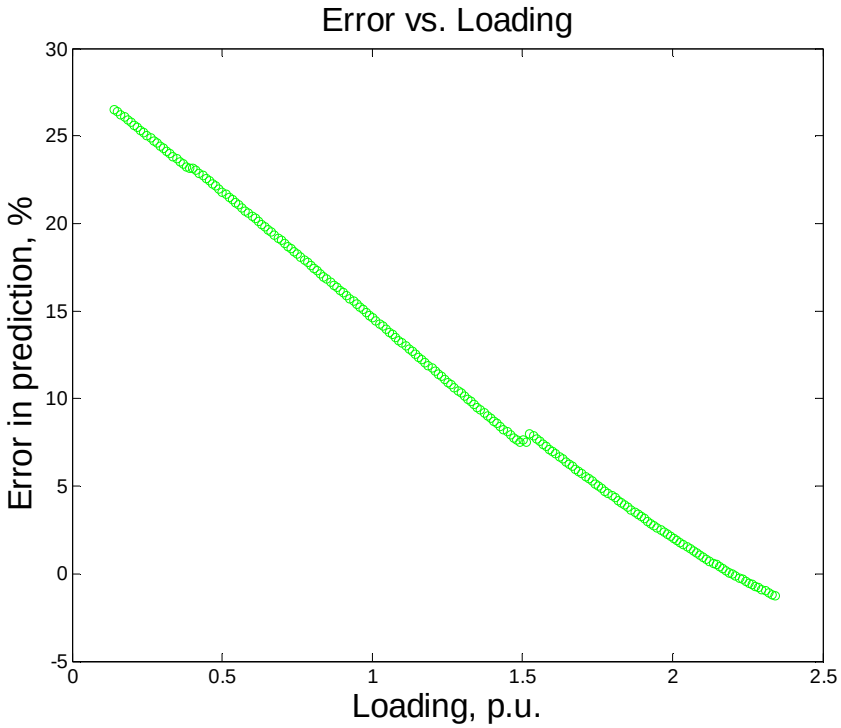

Figure 4.15 Error for IEEE 118 bus system at bus 21, single bus load increase

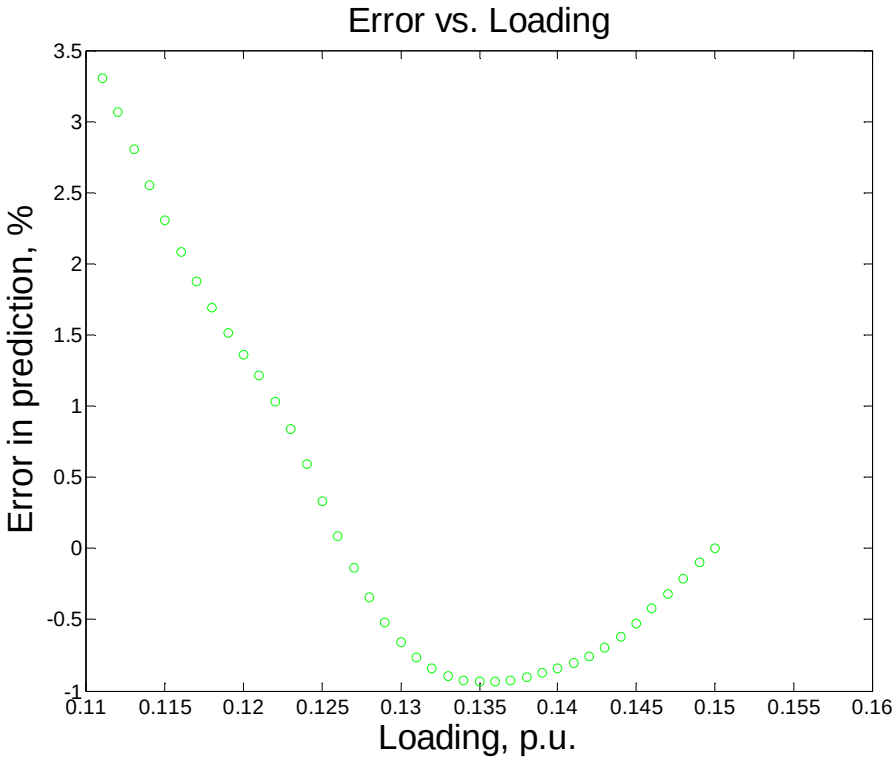

Figure 4.16 Error for IEEE 118 bus system at bus 21, multiple bus load increase

Comparative results between the Thévenin method and the proposed method have been tabulated in Table 4.2. It compares error between Thévenin method and the proposed method for different test systems and loading scenarios. Multiple indicates multiple load increase while single indicates single load increase. One of the main observations to be made from the table is the error offset in the Thévenin equivalent method. The error is not sensitive to closeness to instability. On the other hand, the proposed method causes the error to decrease towards instability and confine it to a very narrow range.

Table 4.2 Error comparison

Test System	**Error Recorded (%)**			
	Thévenin Equivalent		**Proposed Method**	
	Multiple	**Single**	**Multiple**	**Single**
2 bus	-	-156.8 to -156.8	-	7 to -2
5 bus	-270 to -120	-55 to -30	23 to -5	18 to 1
9 bus	-50 to -42	-30 to -15	27 to 2	13 to -1
30 bus	-250 to -100	-60 to -20	25 to 2	30 to -5
118 bus	-300 to -150	-100 to -50	4 to -1	28 to -3

4.6 Conclusion

The consideration of available reactive reserves in computation of voltage stability margin has proven to be very accurate and reliable compared to the Thévenin Equivalent method. The error rate as we approach the loadability limit falls exponentially. The reactive limits of generation or contingencies such as outage of a line influence the reactive loss of a line; however the effect is more benign as compared to Thévenin equivalent. An index calculated from this method would therefore be more reliable. The implementation of VCA determination in the online scenario as explained is feasible. Future work is recommended on techniques to quickly determine the VCA. The proposed method can be extended to online voltage security assessment by considering a set of credible contingencies and by monitoring the smallest margin at any given time.

5 ATTRIBUTE SELECTION FOR ONLINE VOLTAGE STABILITY MONITORING USING DECISION TREES

5.1 Overview

With available wide area measurement system [8], the power system is overflowed with data. Given the accuracy and speed of measurement the setup has been envisaged to be useful in state estimation, feedback control systems, adaptive relaying and security monitoring. The data so obtained is also identified to be a potential source of information for applications such as tracing of system behavior prior and post system wide events, parameter updating for power system models and prediction of angular instability and voltage instability. In this chapter, efficient model development for voltage stability monitoring is discussed and a method proposed. These applications are suitable for online applications because the time consuming calculations are done offline and the decision results are almost instantaneous.

The extraction of implicit, previously unknown, and potentially useful information from data is known as data mining [56]. Although, modern power system has staggeringly high volume of data, the need for data mining applications in power systems can be traced quite far back. The first attempt to apply statistical pattern recognition (PR) to power system security was done by Dy Liacco in the late sixties [57].

The voltage stability monitoring problem is a classification problem. Over the years, commonly used classification algorithms for voltage stability monitoring are artificial neural networks (ANN) [14, 15] and decision trees [11-13]. The advantage of DTs over ANN is that DTs produce easily understood structural descriptions [58]. In other words DTs are transparent methods while ANNs are black box. The usefulness as a result becomes twofold: firstly, we get the classification result and secondly the system

knowledge. For example, by knowing attribute for splitting in a decision tree we can monitor a region associated with that attribute for stability and control functions.

5.2 Motivation

There are numerous studies in implementation of DTs for power system voltage stability monitoring [11-13]. Cutsem et al [11] developed a systematic way to adapt DTs for voltage security monitoring. The importance of candidate attributes has been highlighted but the pre-selection of such attributes has been left to human expertise. Similarly, Nuqui et al [12], proposed a methodology on implementation of DTs for online voltage security monitoring using phasor measurements. The authors propose a new candidate location for an additional PMU so that the overall accuracy of the system is enhanced. This sums up to finding the best attribute for formation of DTs. The problem is solved by considering every other bus to be the candidate location at a time and checking the accuracy of prediction. If this problem was extended to more number of candidate locations then the computational time would rise exponentially. Apparently, we need to look for systematic way to handle the issue. Another study by Vittal et al [13] has similarities on the problem formulation, but presents many variations of use of measurements for voltage stability monitoring. For example, angle differences, reactive power flow in lines, current in lines, voltage drops in lines, square of bus voltages, etc have been used as attributes. The elements chosen are appropriate as voltage stability has relationship to such parameters. However, we should have a systematic method to choose the parameters rather than trying out combinations on hit and trial basis. The solution to this is to select attributes beforehand following a systematic procedure. This chapter deals with developing systematic procedure for attribute selection in decision tree application. One of the challenges in data mining applications is scalability (the size of

the data). There are two ways to deal with this issue. One approach is to develop a more scalable algorithm which is able to handle a large amount of data. Other approach is to engineer the data. Engineering means making the data more compact by eliminating redundancy and insignificant portions using an intelligent technique. [56, 58]

The work in this chapter is focused on improving the data. Specifically, an attribute selection method is proposed. To put things in perspective the following example can be considered. A typical measurement vector of power system is voltage and angle at all buses, real power generation, reactive power generation, real power demand and reactive power demand. With these assumptions, for a four bus system with 2 generators the data vector will have 8 (voltage and angles at each bus) +4 (real and reactive power generation level at each generator) + 8 (real and reactive demands at each bus) = 20 elements. If the problem was to be extended to a real system where the system size is in the order of thousands of buses, the dimensionality (the length of the data vector) of the problem will be daunting. However, most of the data elements are redundant. For example the voltage and angles can be derived from power flow using the given generation and load demands. This observation reduces the data dimension to 8 from 20. Secondly, the generator voltages are not sensitive as they are controlled, so they would not be useful either. Finally only four elements remain in the data. The number of attributes can be further reduced by following appropriate techniques. The previous DT implementations assumed a limited measurement vector from limited PMU locations. However, in the future observability of the entire system can be expected. In addition it might be necessary to identify PMU locations which can be identified by applying attribute selection procedure. There are standard data mining techniques for attribute selection. However, no single method of attribute selection is the best and sufficient. Every method has its own bias. For reliable the outputs of different independent methods have to be considered. This exercise may not necessarily give ‘the global best’ set of

attributes but it will definitely produce better attributes and more general rules. The focus of this work is to see if attributes can be selected based on power system knowledge and the accuracy maintained. The method applied is tangent vector sensitivity [16] of attributes. The significance of this exercise can be listed as follows:

- Reduce the dimensionality of the problem. This saves a lot of offline computation time and resources and also increases the speed of online implementation.
- Using a power system approach to select attributes complements the data mining approaches and makes the results more robust and reliable.
- By limiting ourselves to as little attribute as possible, it will be easy to track them for stability information.
- The information will also be useful in planning. For example future locations for PMUs can be identified.

5.3 Decision Tree

Decision tree is a data representation technique [58]. It consists of nodes and branches. Nodes are the points in a tree where a test is done on the attribute; branches are outcomes of the test that lead to another node. There are three kinds of nodes: root node, internal node, leaf node. Root node is the topmost node, internal nodes are in-between nodes and the leaf node is the end node. The completion of a test is decided by the purity of a node. If a node attains a certain predefined level of class purity then the node is terminated. In order to classify an unknown sample, the attribute values of the sample are tested against the decision tree. A path is traced from the root to a leaf node that holds the class prediction for that sample. The structure and working of a decision tree can be explained using an example. The data, Table 5.1, is the weather nominal data which is

available in Waikato Environment for Knowledge Analysis (WEKA) [59] and corresponding decision tree is shown in Figure 5.1. WEKA is open source machine learning software that has been used for testing the data for attributes on different algorithms in this work.

Table 5.1 Weather data

Outlook	**Temperature**	**Humidity**	**Windy**	**Play**
Sunny	Hot	High	False	No
Sunny	Hot	High	True	No
Overcast	Hot	High	False	Yes
Rainy	Mild	High	False	Yes
Rainy	Cool	Normal	False	Yes
Rainy	Cool	Normal	True	No
Overcast	Cool	Normal	True	Yes
Sunny	Mild	High	False	No
Sunny	Cool	Normal	False	Yes
Rainy	Mild	Normal	False	Yes
Sunny	Mild	Normal	True	Yes
Overcast	Hot	High	True	Yes
Overcast	Hot	Normal	False	Yes
Rainy	Mild	High	True	No

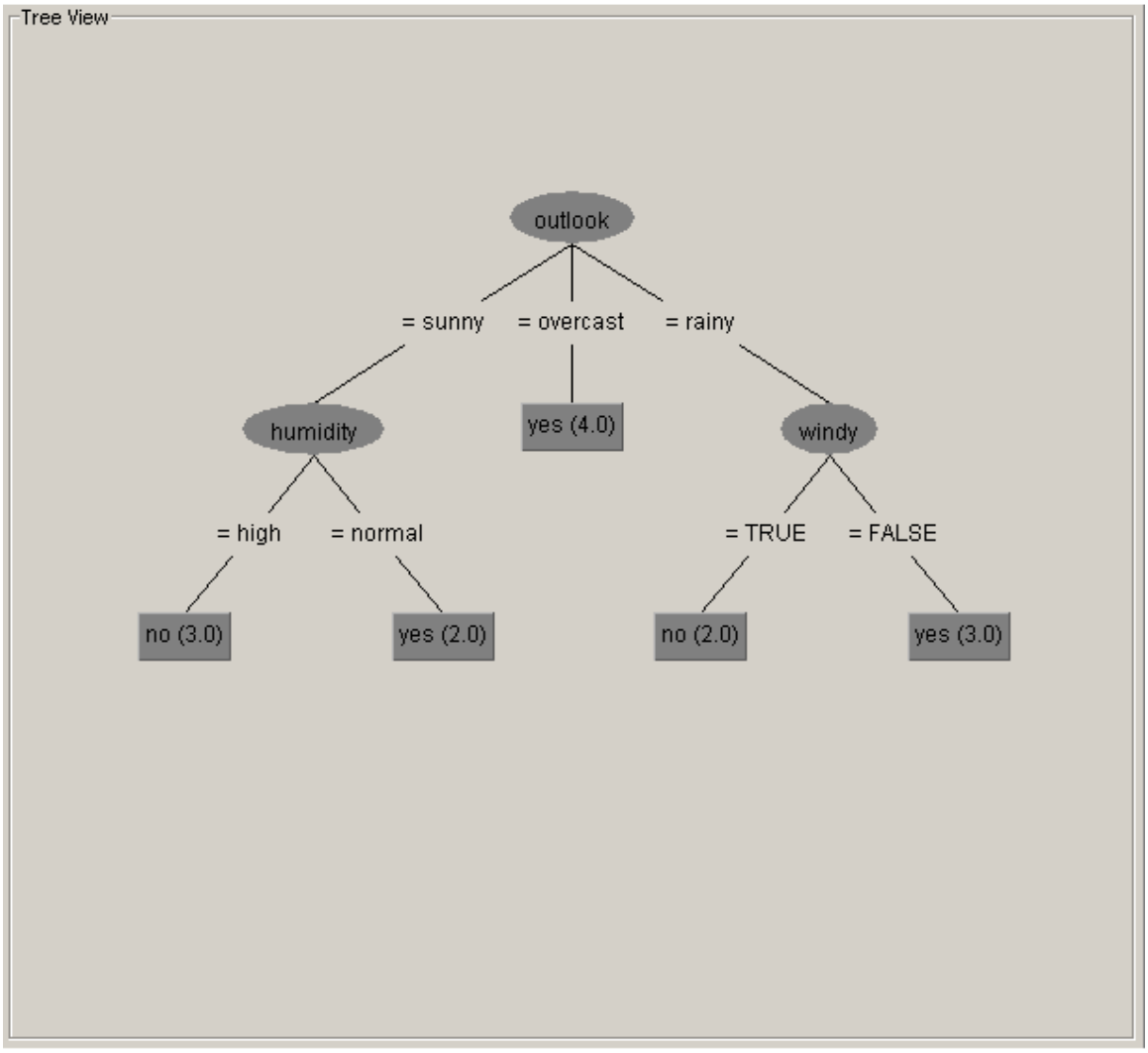

Figure 5.1 Decision tree generated by WEKA for the data given in Table 5.1

The objective of data in Table 5.1 is to decide whether a given day is suitable for playing. Hence, ‘play’ is the class attribute that needs to be predicted. The values that the attribute ‘play’ takes are the class values. In this problem there are two classes to predict, viz. ‘yes’ or ‘no’. All the elements of the first row are the attributes and the values they take listed along the columns are called instances. Since we have discrete instances the attributes are called nominal. If the attributes are continuous set of numbers they are called numeric attributes.

Figure 5.1 is the decision tree output obtained from WEKA. As per the previous definitions, ‘outlook’ is the root node; ‘humidity’ and ‘windy’ are the internal nodes and

the decision nodes are the leaf nodes which contain the classes. It is seen that the leaf nodes have single attribute values such as ‘yes’ or ‘no’. During the formation of decision tree, an attribute for a node is decided based on its ability to reduce the impurity of the division that it produces on a dataset. The algorithm [58] used to build the decision tree in Figure 5.1 measures the impurity reduction by calculating entropy and expected information which has been explained in the following section.

5.3.1 Decision Tree Building

The basic task in building a DT is to find an attribute to be tested on a node and branching to another node repeatedly. The process of finding an attribute for a test and branching is called splitting. The objective of a split in a tree is to reduce the impurity in the dataset with respect to class in the next stage. [58]This can be accomplished by information gain measure. The calculation is done in two stages. First the entropy of the dataset is measured and using this value expected information gain is calculated. The entropy of a dataset is given by expression 5.1.

$$Entropy(S) = \sum_{i=1}^{c} -p_i log_2(p_i) \qquad 5.1$$

Where,

c= number of classes

S= training data (instances)

p= proportion of S classified as i

In the second stage, expected information gain is calculated which is given by expression 5.2.

$$Gain(S, a) = Entropy(S) - \sum_{v \in values(a)} \frac{|S_v|}{|S|} Entropy(S_v) \quad 5.2$$

Where,

$$S_v = \{s \in S : a(s) = v\}$$

v= value of the attribute.

Gain(S,a) is the expected information gain obtained from the knowledge of attribute 'a'.

For the dataset in Table 5, using equation 5.1,

$$Entropy(S) = \sum_{i=1}^{c} -p_i log_2(p_i)$$

$$= -\frac{9}{14} log_2 \frac{9}{14} - \frac{5}{14} log_2 \frac{5}{14} = 0.94$$

Similarly for instances of the attribute 'outlook' the entropies are as follows:

$$Entropy(S_{sunny}) = 0.97$$

$$Entropy(S_{overcast}) = 0.00$$

$$Entropy(S_{rainy}) = 0.97$$

Now the expected information gain is calculated using equation 5.2.

$$Gain(S, outlook) = Entropy(S) - \sum_{v \in values(a)} \frac{|S_v|}{|S|} Entropy(S_v)$$

$$= 0.94 - \frac{5}{14}.0.97 - \frac{4}{14}.0 - \frac{5}{14}.0.97$$

$$= 0.94 - 0.69 = 0.23$$

Similarly computation of expected information gain of other attributes yields,

$$Gain(S, temp) = 0.03$$

$$Gain(S, humidity) = 0.15$$

$$Gain(S, windy) = 0.05$$

The expected information gain is the highest by choosing the attribute ‘outlook’ which is 0.23, so it is chosen as the root node as seen in Figure 5.1. The attribute outlook has 3 instances; hence the three branches. The next step is to find the attribute for the next node after branching. Consider the branch ‘sunny’. The dataset is now confined to all the instances which have ‘outlook’ to be ‘sunny’. The total number of instances in the dataset reduces to 5. Within these 5 data points, the attribute ‘outlook’ is not considered. The entropy and expected information gain is calculated for rest of the attributes.

Thus,

$$Entropy(S) = \sum_{i=1}^{c} -p_i log_2(p_i)$$

$$= -\frac{2}{5} log_2 \frac{2}{5} - \frac{3}{5} log_2 \frac{3}{5} = 0.97$$

For the attribute temperature entropy for its instances,

$$Entropy(S_{hot}) = 0$$

$$Entropy(S_{mild}) = 1$$

$$Entropy(S_{cool}) = 0$$

The temperature information gain:

$$Gain(S, temp) = Entropy(S) - \sum_{v \in values(a)} \frac{|S_v|}{|S|} Entropy(S_v)$$

$$= 0.97 - \frac{2}{5}.0 - \frac{2}{5}.1 - \frac{1}{5}.0 = 0.57$$

Similarly,

$$Gain(S, humidity) = 0.97$$

$$Gain(S, windy) = 0.02$$

Finally, the information gain is highest for the attribute, 'humidity' along the branch 'sunny'. As a result it becomes the second node. By repeating the calculations for other branches and nodes the entire tree is induced.

5.3.2 Issues with the Tree

The kind of approach pursued in developing the above tree is the greedy search. That is because the decision is based on what is best now and future nodes are not being considered. Genetic algorithms [43] help in searching for the global optimum subset.

In Figure 5.1 the decision tree correctly classifies every instance. Although this seems to be a good solution for the training dataset, the classifier may not do well with other datasets. This is a case of over fitting [58]. Over fitting makes the tree large and complex (hence requires a lot of computation time) and will not be able to generalize the rules (the model will not produce good results for an independent test set). Over fitting becomes a nuisance when the data is contaminated by noise and outliers. A solution to

this problem is to prune a tree. Operations such as pre-pruning and post-pruning are done to reduce the over fitting effects. To neutralize overfitting, testing should be done using holdout procedures for limited data or by using an independent test set as far as applicable.

. The real world applications have large amounts of data to be handled; hence scalability becomes another prime issue. The strategy is to either increase resources for computation or adapting algorithms with better scalability features. Yet another strategy is to reduce the data. Data reduction can be accomplished by data compression, numerosity reduction and dimensionality reduction. The data compression is the process of transformation of data to a reduced or “compressed” representation of the original data. The numerosity reduction finds a smaller form of data representation. These methods are independent of the system under study.

The third form of data reduction is the dimensionality reduction. This is the process of eliminating the attributes that are not significant for decision tree modeling. Generic mathematical means can be used to filter the attributes but at the same time system information can be also useful. In other words, for attribute selection in power system, knowing the nature of the variables can be of significance. In this thesis, the filtering of attributes is done using data mining algorithms as well as knowledge from power system studies. The study is focused on applicability of power system knowledge for attribute selection.

5.4 Methods of Attribute Selection

There are a large number of attribute selection methods [56, 58]. WEKA, for example has 12 algorithms for the purpose. The outcome of the algorithms may not necessarily be the same. An attribute may be qualified as good by some method while

some other method may give it a very small weight. In such a case, it is necessary to have a combined evaluation of different methods so that in effect the bias of the attribute selection algorithm is nullified. For this reason we want to select attributes using methods that have different discriminating philosophy. In accordance with this line of thought the following attribute selection methods were chosen from WEKA.

- Gain ratio attribute evaluation
- Relief attribute evaluation
- Wrapper subset evaluation using Naïve Bayes learner

5.4.1 Gain Ratio Attribute Evaluation

The information gain of an attribute is given by equation 5.2. This relation biases towards higher number of branching. For example, if there was an extra attribute 'id code' as shown in Table 5.2, this attribute would have the highest information gain and it would be chosen as the root node [58]. With all its branches, all the instances would be perfectly classified, even if all other attributes were ignored. The final outcome would be a tree without any system information. To avoid this situation, attributes are selected according to their information gain ratio. Information gain ratio is given by equation 5.3.

$$Gain\ ratio = \frac{information\ gain}{information\ considering\ daughter\ nodes}$$

$$= \frac{Entropy(S) - \sum_{v \in values(a)} \frac{|S_v|}{|S|} Entropy(S_v)}{Entropy\ (S_{v1}, S_{v2} \dots S_{v3})} \qquad 5.3$$

The denominator takes into account just the number and sizes of the daughter nodes without taking into account the information of the class. With this new

formulation, considering the data in Table 5.2, information gain for the ‘id code’ attribute is 0.94 while the information gain ratio=0.246. For the attribute ‘outlook’, information gain=0.247 while the information gain ratio=0.156. Although the hypothetical attribute ‘id code’ is still preferred, the bias is greatly reduced. The information gain ratio technique ignores attributes having high amount of intrinsic information. To compensate for this, there is a practice of choosing an attribute such that the information gain of that attribute is at least as great as the average information gain for all the attributes.

Table 5.2 Weather data with the ID code attribute

ID code	**Outlook**	**Temperature**	**Humidity**	**Windy**	**Play**
a	Sunny	Hot	High	False	No
b	Sunny	Hot	High	True	No
c	Overcast	Hot	High	False	Yes
d	Rainy	Mild	High	False	Yes
e	Rainy	Cool	Normal	False	Yes
f	Rainy	Cool	Normal	True	No
g	Overcast	Cool	Normal	True	Yes
h	Sunny	Mild	High	False	No
i	Sunny	Cool	Normal	False	Yes
j	Rainy	Mild	Normal	False	Yes
k	Sunny	Mild	Normal	True	Yes
l	Overcast	Hot	High	True	Yes
m	Overcast	Hot	Normal	False	Yes
n	Rainy	Mild	High	True	No

5.4.2 Relief Attribute Evaluation

The relief algorithm evaluates the worth of an attribute by repeatedly sampling an instance and considering the value of the given attribute for the nearest instance of the same and different class (WEKA help). This is an instance based learning approach; specifically the k-nearest neighbor algorithm is tailored to calculate the weight of an attribute. One simple version of the mechanics of the algorithm can be explained as follows [58].

Once the training instance is classified, the most similar exemplar or the most similar exemplar of each class (exemplar is a representative instance of a class) is used as the basis for updating. Let x be the training instance and y the exemplar. For every attribute 'i', the difference $|x_i - y_i|$ is a measure of the contribution of that attribute to the decision. Smaller difference means, the attribute contributes positively where as for a larger distance the attribute contributes negatively. Given the situation, if the classification is correct, the attributes with smaller difference turn out to be important and hence its weight is increased. On the other hand if the classification is incorrect, the weight is decreased. The selection approach is different here from the information gain ratio method as relief attribute evaluation deals with a portion of data rather than the whole data. The number of exemplars used can be more than one (k).

5.4.3 Wrapper Subset Evaluation Using Naïve Bayes Learner

The previous algorithms rank the attributes by a greedy approach. The combination of attributes is not considered. For a selection of 'n' attributes, the combination of top ranked attributes may not necessarily give the best outcome. In order to have a better selection of attributes in a collective sense this approach is followed. The

number of attributes to form a subset is decided and the model is induced using a learning algorithm on the subset. The resulting model is then evaluated. Once sufficient subsets have been tested, the subset with the best results gives the list of selected attributes. Exhaustively trying all the possible combinations can be computationally burdensome, hence search algorithm such as genetic algorithms are used to get the optimum subset. Naïve Bayes is chosen as the learning algorithm as it is different from the above two methods. The method is based on probability theory and has the assumptions of the attributes being class conditional independent. Hence dependent attributes are filtered out. The Naïve Bayes algorithm works as follows:

- Consider a data sample having 'n' attributes and 'm' classes. Given an unknown data sample, X, the class prediction is based on highest posterior probability conditioned on X. The sample X is assigned to class C_i if and only if

  $$P(C_i|X) > P(C_j|X) \; for \; 1 \leq j \leq m \, , j \neq i$$

- We need to maximize the posterior probability to get the class. The posterior probability can be calculated using the Bayes theorem as in equation 5.4:

  $$P(C_i|X) = \frac{P(X/C_i)}{P(X)} P(C_i) \qquad 5.4$$

  In equation 5.4, the denominator is constant for all classes, while $P(C_i)$ can be easily calculated. For the term $P(X/C_i)$, to reduce the computations the naïve assumption here is that the attributes are class conditional independent. Thus $P(X/C_i)$ can simply be calculated using equation 5.5:

  $$P(X/C_i) = \prod_{k=1}^{n} P(x_k|C_i) \qquad 5.5$$

  Now, $P(x_k|C_i)$ can be estimated from the training samples.

5.5 Power System Point of View of the Attributes

The data mining techniques for attribute selection that have been explained in the previous sections are pretty standard. The idea of this thesis is also to use power system knowledge for the selection of attributes. The attributes are selected using values in the tangent vector. The method is based on the hypotheses that attributes sensitive towards system scenarios are the critical attributes for classification. This is reasonable because, if an attribute does not change it is most unlikely that it will discriminate system conditions. For example, voltage of a voltage controlled bus is a bad attribute as it hardly changes, while voltage and angles of electrically distant buses (weak ones) from the reactive and real power source change and those values may be good for predicting classification.

The general procedure of sensitivity analysis is to define a stability index and study its variation with power system parameters such as voltage, angles, loads, contingencies and others [16]. Modal analysis [5] is an example of such type of measure. A voltage stability index based on minimum eigenvalue of the load flow Jacobian is defined. In the second step, sensitivities of different power flow elements such as buses, lines, generators to that eigenvalue (or a mode) is calculated in the form of participation factor.

In a second method, the sensitivities of power system parameters such as voltage, angles are directly calculated with respect to power system loading. This sensitivity is called parametric sensitivity. The information can be used for stability analysis because voltage and angles tend to have high value of sensitivity when the bus associated with them is in the course of collapse. This can be observed in PV diagram (Figure 2.2) where the slope of the PV curve is higher towards the collapse point. In general, when the sensitivity of a parameter towards power system loading is high, it implies that the

parameter is associated with the weaker part of the network and requires corrective actions.

Parametric sensitivity is more suited for attribute selection. This is because the value of the sensitivity suffices in ranking the attributes without any additional computation for stability index. The sensitivity information is obtained from tangent vector [16]. More details on tangent vector evaluation are given in section 5.8. The tangent vector elements are differential changes in bus voltage angles ($d\delta_i$) and magnitudes (dV_i) with respect to differential change in loading ($d\lambda$). Hence the tangent vector elements serve as the voltage and angle sensitivity with respect to loading. These parameters are the attributes of the decision tree model.

5.6 Decision Tree Implementation in Voltage Stability Monitoring

Figure 5.2 gives a general picture of the real time application of decision tree in voltage stability monitoring. Once the credible contingencies, operating conditions and scenarios are known, the next step is to generate a data base. The database is used to build a decision tree model. The tree, on real time will give the stability information when fed by a measurement vector.

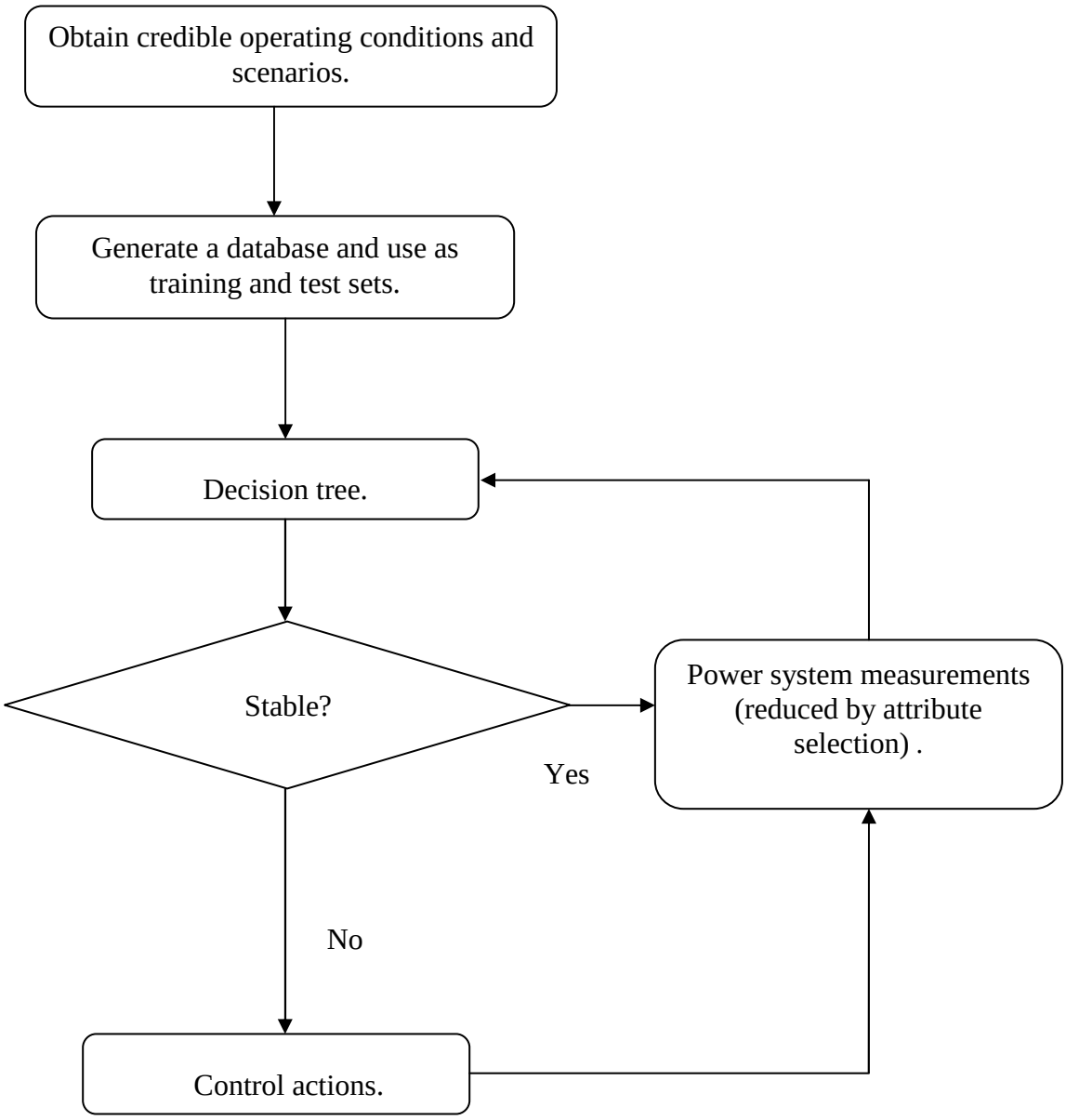

Figure 5.2 Implementation of decision tree in voltage stability monitoring of power system

5.7 Data Generation

Ideally, the results would be of more significance if the data was from direct field measurements. It is highly possible that, the data obtained from simulated environment lack the exact representation of system state and may be biased with respect to assumption of load variations and scenarios. Engineering judgment is useful in such a case. The advantage of having simulated data is in getting a great variety of data within a very short span of time. Possibly, getting the real life data with as much variety would require years of data collection.

Data is required to train and test the decision tree model. Training set is used to make classification rules. Test set is used to check accuracy of the model. Depending upon the availability of data, there are various holdout procedures as cross validation, leave one out and bootstrap to use for model validity [58]. In this study an independent test set has been used.

In order to know the system conditions to vary in generating the data, it is essential to know the parameters that impact voltage instability or the voltage stability margin. Following parameters are seen to vary voltage stability margin [2]:

- Load increasing scenario
- Generation dispatch
- Contingencies

The influence of above variations on voltage stability margin is demonstrated by PV curves of Figures 5.3a and5.3 b. Figure 5.3a demonstrates the voltage stability margin variation with different scenarios (defined by contingencies and load increments). Figure 5.3b has varying base points (defined by different load allocations and generation dispatch) but the same scenario, yet margins differ.

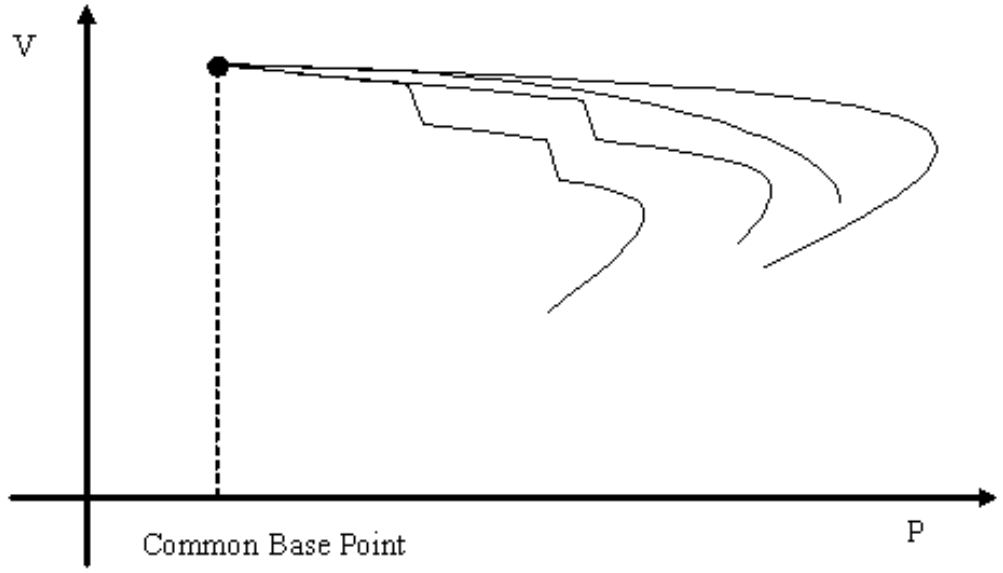

Figure 5.3a Change of voltage stability margin with respect to different scenarios

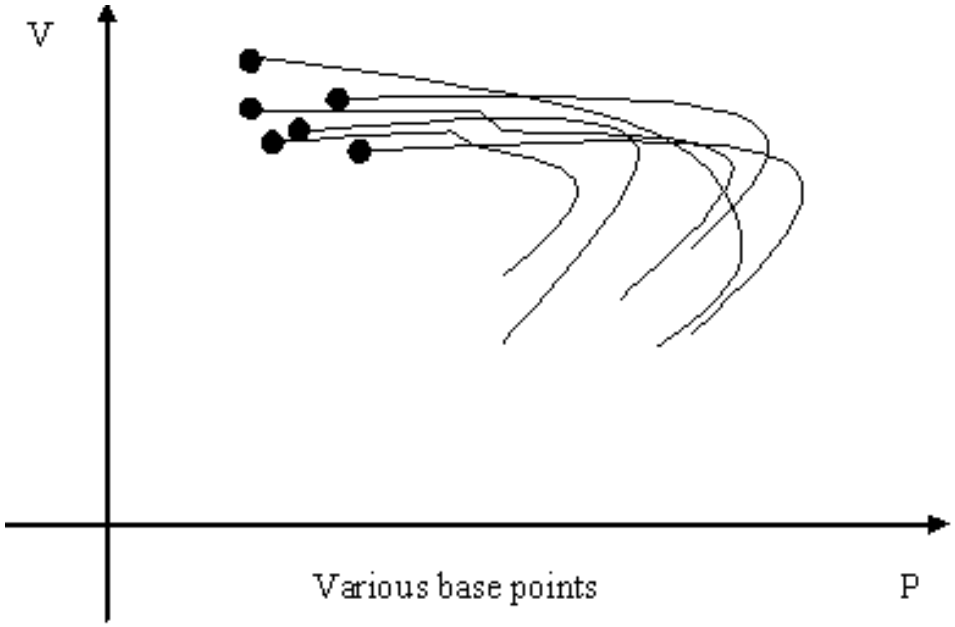

Figure 5.3b Variation of voltage stability margin with variation of base points

While generating data load increase scenario is realized by randomizing the base loading and increasing the load in their corresponding proportion. The generation dispatch variation is performed by randomizing the generation. All line outages are

considered as credible contingencies. While increasing the load, the generation is proportionally divided among the generators according to their base generation so that the slack generator doesn't have to bear the entire load increment, which otherwise would be unrealistic.

5.7.1 Voltage Stability Criteria

There is not a universal approach to voltage security classification [12]. Commonly followed approaches seek for minimum or maximum threshold for voltage magnitude at different buses and possibly different specific values for buses identified as important ones. Further, an operating point is defined as 'secure' based upon the available real power margin. Real power margin is simply additional real power that can be loaded to the system before collapse. This is defined in percentage of the peak load. For example minimum voltage should be greater than 0.92 p.u. and margin to voltage collapse of 12.5 % for a stable case [12].

In this study, an operating condition is assumed to have three classifications: secure, alert and insecure. The percentage of margin considered for this test is as follows: if the system is within 10% then the system is considered insecure, if the margin is between 10-20 % the system is said to be in alert stage while margin > 20% means a secure state. The buffer zone of alert stage gives the operator, time to decide on control actions in case the system is to enter the insecure state. The criterion is illustrated by Figure 5.4.The secure state is a green light for the operator, insecure is the red light and the alert state is the orange light. In order to find the outcome of an operating condition for a given scenario, the test system is stressed accordingly until the end point. Once the outcome is known, the data vector is stored in an .xls file. This data vector consists of voltages and angles of all the buses and the classification value: secure, insecure or alert

state. The next phase is to input the data in WEKA for further analysis which will be covered in the results and analysis section.

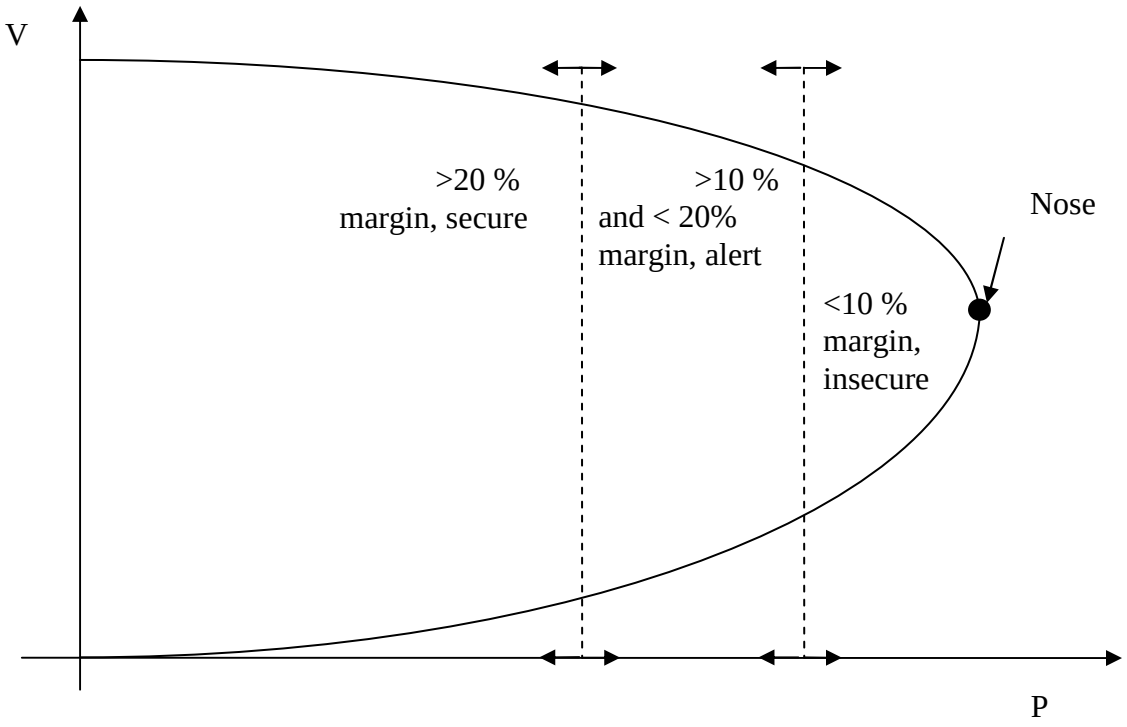

Figure 5.4 Security criteria

5.7.2 Test System

The test system used for data generation is IEEE 30 bus system (Figure 4.15). The system data is available in Matpower package that runs in Matlab, which are open source codes. Sampling for random numbers is done using a normal distribution using the Matlab function ‘random’. To be specific with the experiment performed here: There are 6 random generator dispatches, 5 random loading conditions and 38 contingences. The base case loading is 272 MW and the peak loading is of 490 MW implies approximately 50 MW as 10% of the peak load. This number could vary for contingent conditions- most likely a smaller value. For unsolvable cases obtaining the nose point becomes an iterative process. To reduce the computation, the loading was reduced by 35 MWs flatly in all cases as a representation of the insecure state, 70 MW for the alert case and margins of 150 MW considered the secure state. Using the MWs instead of percentage randomizes the portion of the PV curve from which the sampling is done within the percentage limits. If a constant percentage is taken as the margin then there is a possibility that we sample around the same section of the PV curve. For each scenario, 3 observations are taken to represent the three classes. Thus we have approximately 6×5×38×3 =3420 data points. Out of which nearly 1000 points are taken as a test set and the rest is used for training the decision tree.

Figure 5.5 is the flow chart for data generation process. A part of the data is available in Appendix A.

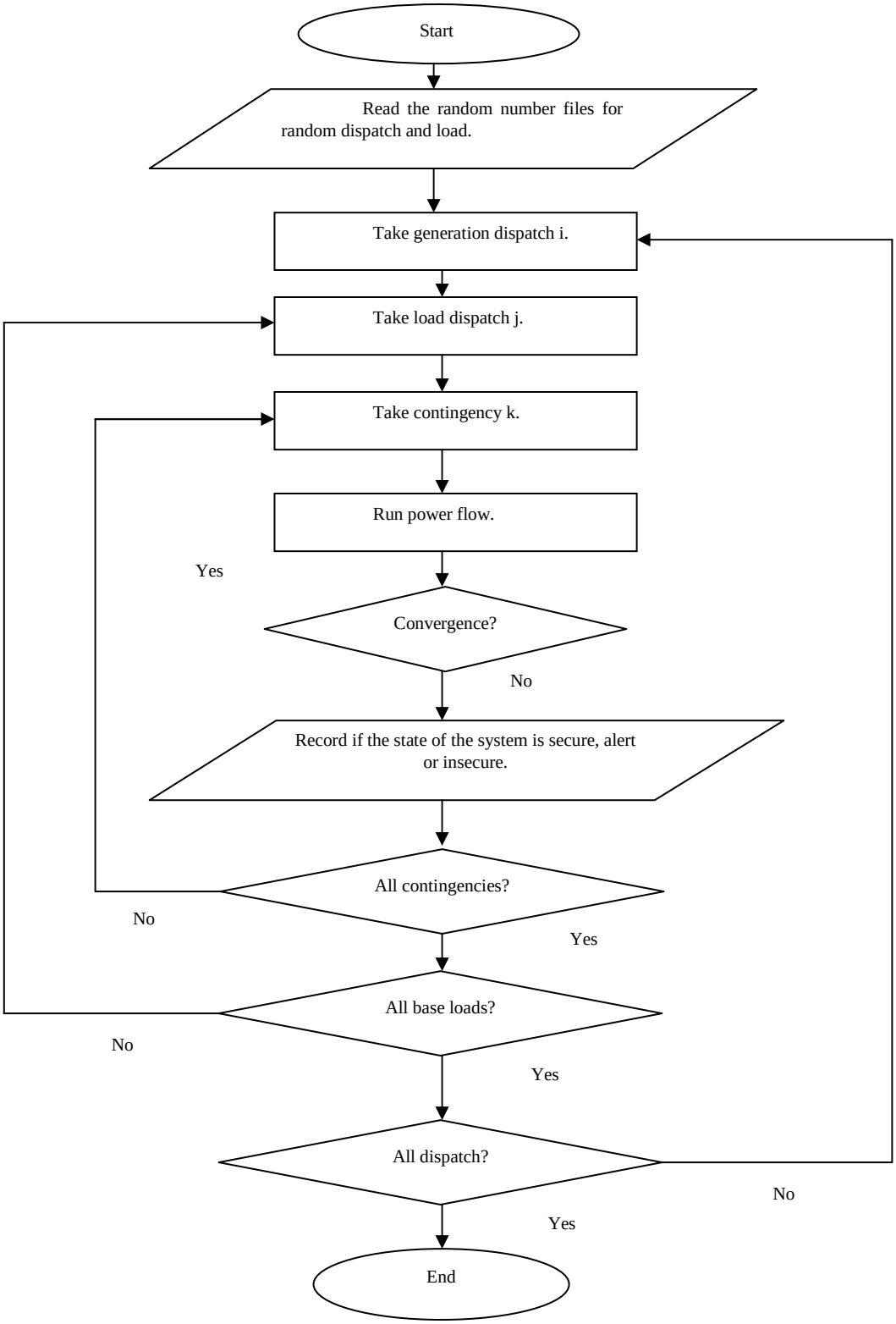

Figure 5.5 Data generation for decision tree modeling

The correct size of the dataset is a very important aspect in DT induction. DTs, for a smaller dataset can be prone to instability resulting in trees with varying structure and accuracy for slight perturbation [60]. The perturbation could be in the form of change in attribute values or in the number of instances. In order to test the stability of DT in the learning set, the data was divided into 10 folds. Only 9 folds were taken at a time to induce a DT. The generated DT was tested against an independent dataset. This is the 10 fold cross validation technique [58].The outcome is presented in Table 5.3. The accuracy ranges from 95% to 98% while the size of the tree varies very slightly as shown. The results imply that size of the dataset considered is sufficient in terms of stability of DT induction.

Table 5.3 Stability evaluation of DT for the generated dataset

Fold Removed	**Size of the Tree (number of nodes)**	**Accuracy (%)**
1	170	96.0
2	178	96.8
3	178	96.8
4	178	96.9
5	185	97.6
6	178	96.8
7	175	96.8
8	182	95.0
9	175	97.6
10	180	97.8
none	177	97.6

5.8 Tangent Vector Calculation

The method for tangent vector calculation is l explained in Chapter 2 (section 2.2.1.1). The tangent vector gives the sensitivity of the parameters at a point in the PV curve where they are evaluated. Since we want to classify a given operating state as secure, alert or insecure, the attributes should be such that they predict each of these categories accurately. Hence sensitivities in the entire region of the PV curve should be evaluated. Here, the samples were taken within 10%, 10 to 20% and >20% of the PV curve from the end point. The tangent vector was calculated for every credible contingency (here the line outages). Since the angle and voltage sensitivities are not comparable, they have been ranked separately and 50% of each category is input in the final set. For example to select 20 attributes, top 10 attributes come from angle sensitivities and the rest from the voltage sensitivities. Because the tangent vector elements are negative and sensitivity is considered to be based on magnitude, normalized magnitude of sensitivities is taken for comparison [16]. Figures 5.6 and 5.7 are the bar plots of the actual values of the top three attributes from the angles and voltages respectively for different operating conditions for various contingencies. The corresponding sensitivity values are tabulated in Tables 5.4 and 5.5 respectively. It is seen (Figure 5.6- sensitivities for conditions 2, 3, 4) that sensitivities are different for different operating conditions. This indicates the nonlinearity of the PV curve. Even with this non linearity the general trend of the sensitivity was such that the relative ranking of the attributes remained the same irrespective of system conditions. This is consistent with the results obtained in [16] for the 39 bus system. The sensitivities at lighter loads were found to be smaller compared to the stressed conditions. The peaked bars (having higher values) in Figures 5.7 and 5.8 are for the stressed conditions. The tangent vectors were

evaluated for IEEE 118 bus system. The sensitivity trend was found to be similar to the one observed for IEEE 30 bus system.

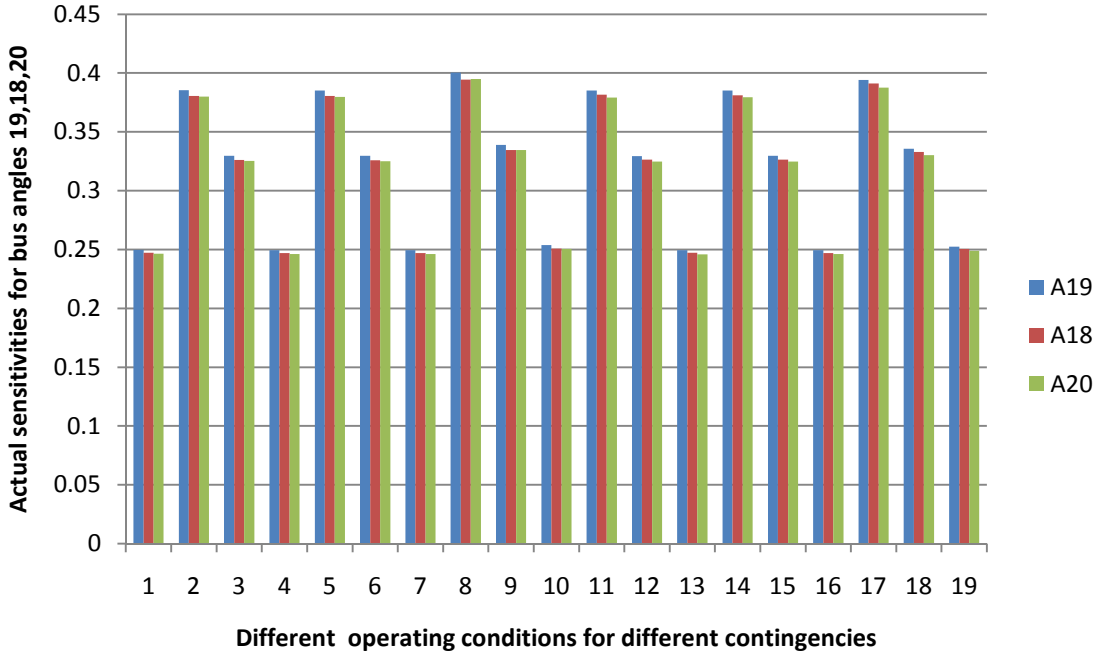

Figure 5.6 Part of angle sensitivities for buses 18, 19 and 20 (top three angle attributes)

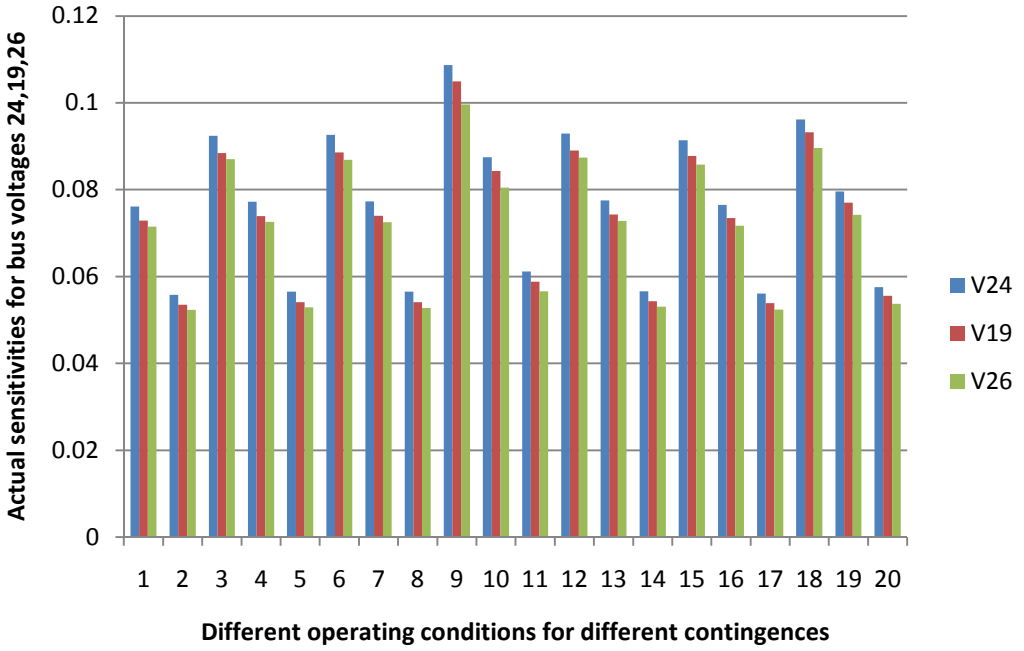

Figure 5.7 Part of voltage sensitivities for buses 24, 19, 26 (top three voltage attributes)

Table 5.4 List of angle sensitivities for plot of Figure 5.7

Some System Condition	Angle Sensitivities (in the order of top ranks, actual values)			Corresponding sensitivities (normalized values)		
	A19	A18	A20	A19	A18	A20
1	0.3302	0.3267	0.3256	1	0.9894	0.9861
2	0.2497	0.2472	0.2464	1	0.9901	0.9867
3	0.3853	0.3806	0.3799	1	0.9879	0.986
4	0.3297	0.326	0.3252	1	0.9887	0.9864
5	0.2495	0.2469	0.2462	1	0.9896	0.9869
6	0.3852	0.3806	0.3797	1	0.9882	0.9858
7	0.3296	0.3259	0.3251	1	0.9888	0.9863
8	0.2494	0.2469	0.2462	1	0.9897	0.9868
9	0.4003	0.3944	0.3948	1	0.9852	0.9863
10	0.339	0.3345	0.3345	1	0.9866	0.9867
11	0.2537	0.2507	0.2505	1	0.9883	0.9872
12	0.3851	0.3815	0.3792	1	0.9907	0.9846
13	0.3295	0.3265	0.3247	1	0.9909	0.9853
14	0.2494	0.2472	0.2459	1	0.9911	0.9861
15	0.3851	0.381	0.3794	1	0.9895	0.9852
16	0.3296	0.3263	0.3249	1	0.9899	0.9857
17	0.2495	0.2471	0.2461	1	0.9905	0.9864
18	0.3941	0.391	0.3875	1	0.9921	0.9832
19	0.3356	0.3329	0.3303	1	0.992	0.9842
20	0.2525	0.2505	0.2488	1	0.992	0.9854

Table 5.5 List of voltage sensitivities for plot of Figure 5.8

Some System Condition	Voltage Sensitivities (in the order of top ranks, actual values)			Corresponding sensitivities (normalized values)		
	V24	V19	V26	V24	V19	V26
1	0.0761	0.0729	0.0715	1	0.9582	0.9389
2	0.0558	0.0535	0.0523	1	0.9587	0.9363
3	0.0924	0.0884	0.087	1	0.9565	0.9416
4	0.0772	0.0739	0.0726	1	0.9569	0.94
5	0.0565	0.0541	0.0529	1	0.9575	0.9375
6	0.0926	0.0886	0.0869	1	0.9577	0.9391
7	0.0773	0.074	0.0725	1	0.9579	0.9379
8	0.0565	0.0541	0.0528	1	0.9583	0.936
9	0.1087	0.1049	0.0996	1	0.9651	0.9157
10	0.0875	0.0843	0.0805	1	0.9635	0.9199
11	0.0612	0.0588	0.0566	1	0.9616	0.9247
12	0.0929	0.089	0.0874	1	0.9578	0.9408
13	0.0775	0.0743	0.0728	1	0.9581	0.9392
14	0.0566	0.0543	0.0531	1	0.9584	0.9368
15	0.0914	0.0878	0.0858	1	0.9605	0.9382
16	0.0765	0.0735	0.0717	1	0.9603	0.937
17	0.0561	0.0539	0.0524	1	0.9601	0.935
18	0.0962	0.0932	0.0896	1	0.9693	0.9314
19	0.0796	0.077	0.0742	1	0.9672	0.9317
20	0.0576	0.0556	0.0537	1	0.9646	0.9316

5.9 Results and Analysis

In this section, attributes selected from different methods have been compiled and analyzed. The entire space of attributes consists of real and reactive power injections and voltage and angles at all buses. Only voltage and angles are considered for further processing. This is because voltages and angles are readily available from the phasor measurements. Interestingly, it was observed that using voltage and angles gave better results compared to real and reactive power injections. Further, real and reactive power

injections are dependent on angles and voltages. Consequently there is a little chance that information is lost.

The data was inputted as .CSV (comma separated value) file to WEKA. Very minor data preprocessing such as discretization was done. This would relieve computational load in building the decision tree model. Table 5.6 gives the top 20 attributes selected by different methods. The gain ratio, relief and tangent vector methods rank the attributes. The columns corresponding to those methods give the ranked list. The rank for angles and voltages apply separately for the tangent vector attribute selection. The column corresponding to the subset evaluation is not a ranked list. The alphabet 'A' stands for angle and 'V' stands for voltage. The numbers following them represent the bus number. Table 5.7 gives the accuracy obtained in the models built from different attribute selection procedure and the time taken for each model. It is seen that prediction accuracy from tangent vector selection procedure is highest among the different filters. The farthest column on the right is the accuracy of the model when all the attributes are selected. It has the highest accuracy, but not of appreciable incremental value. Time taken to build the model is 30ms compared to other methods which only take 20ms. The time factor can be very significant for periodic update of the models in the online paradigm for large interconnections where the number of buses in the network is in the order of thousands.

The final selection of the 20 attributes was done based on their occurrences (repetitions/votes) and the ranks they held (in case of conflicts, since the pool has more than 20 attributes). The outcome is shown in Table 5.8. The first column is the pre-selected attributes with more than one vote, the second column is their corresponding votes, the third column is the finally selected attributes and the fourth column is the accuracy obtained. The accuracy is the highest (98.14%) of all the cases considered until now (Table 5.7). This has been accomplished by a much smaller set of attributes (20)

versus considering all the attributes (53, the case that had the highest accuracy previously). This outcome is likely because when attributes are not filtered, the insignificant and redundant attribute, can gain importance deep down the tree. As a result, the tree tends to be less general and is likely to perform worse in an independent test set.

As a further test on the selected attributes of Table 5.8, different subsets were considered for accuracy. In Table 5.9 first row consists of attributes with the highest number of votes. There are three such attributes. Next row has 3 votes for each attributes. The third row is the combination of the two. In the fourth row attributes with two votes were considered while the attributes in the fifth set are the ones that have been considered unimportant by the selection methods. It is found that, the seven attributes in the third row has as high accuracy as 97.8%. This accuracy is comparable to the one obtained from 20 selected attributes. Thus there is a further reduction of the final set of significant attributes. The voting system as seen from Table 5.9 has worked well for the available data. The accuracy from attributes that were considered unimportant (Table 5.9, row 4) is 82.06 %. This accuracy is low although more number of attributes has been considered. Thus, properly selected attributes improve the model accuracy rather than a large set of unfiltered attributes.

Table 5.6 Attributes selected by different methods

Method / Rank	Gain Ratio	Relief	Wrapper (Naïve Bayes)	Tangent Vector
1	V17	A8	V1	V24
2	V15	A9	V11	V19
3	V20	A11	V15	V26
4	V16	A6	V18	V20
5	V19	A7	V19	V18
6	V14	A28	V24	V23
7	V18	A3	V26	V21
8	V24	A4	V28	V22
9	V25	A1	V29	V25
10	V30	A2	A1	V17
11	V22	V19	A2	A19
12	V21	A16	A7	A18
13	V29	A12	A8	A20
14	V23	V18	A9	A23
15	V10	V14	A12	A21
16	V12	A13	A17	A14
17	V26	A17	A20	A15
18	V27	V17	A22	A22
19	A8	A14	-	A24
20	A6	V24	-	A17

Table 5.7 Accuracy from different set of attributes

Attributes Selection method	**Gain Ratio**	**Relief**	**Wrapper**	**Tangent vector**	**All Attributes**
Accuracy (%), J48 algorithm used	96.7	91.75	96.39	97.3	97.63
Time to build the model (ms)	20	20	20	20	30

Table 5.8 Final attribute selection (top 20)

Attributes	**Occurrences/votes in sets obtained by selection algorithms**	**Selected Ones (top 20)**	**Accuracy (%)**
V14	2	V14	
V15	2	V15	
V17	3	V17	
V18	4	V18	
V19	4	V19	
V20	2	V20	
V21	2	V21	
V22	2	V22	
V23	2	V23	
V24	4	V24	
V25	2	V25	
V26	3	V26	98.14
V29	2	A1	
A1	2	A2	
A2	2	A9	
A6	2	A13	
A7	2	A16	
A8	3	A17	
A9	2	A20	
A12	2	A22	
A14	2	-	
A17	3	-	
A20	2	-	
A22	2	-	

Table 5.9Accuracies for different sub sets of attributes based on number of votes

Attributes	Occurrences/Votes	Accuracy (%)
V18, V19, V24	4	90.6
V17,V26, A8, A17	3	93.5
V18, V19, V24, V17,V26, A8, A17	4/3	97.8
V1,V2,V3,V4,V5,V6,V7,V8,V9,V10,A5, A10, A27	0	82.06

Finally, most of the attributes selected are associated with buses 14,17,18,19,20,21,22,23,24,25,26 which are load buses that are located distantly (electrical distance) from the real and reactive power sources (Figure 4.15). This is crucial information as weak buses need to be monitored to have an understanding of the stability of the system. This weak area identification can be further investigated to determine whether the data mining algorithms consistently select attributes related to weak buses.

5.8 Conclusion

A systematic procedure to select attributes for decision tree modeling has been presented. The method considers data mining techniques as well as the engineering point of view of the power system for attribute selection. This opens application s for different other voltage stability analysis techniques for attribute selection and research on finding better techniques. Another observation is that, the attributes associated with weak areas have a significant role in classification. This implies that statistical and data mining techniques have the potential for weak area identification in power system.

6 Conclusion and Future Work

6.1 Conclusion

This thesis gives a synopsis of online voltage stability monitoring. Current practices in online monitoring have been presented along with their drawbacks. The current approach to the problem consists of application of online measurements and stored data. For the first method, use of Thévenin equivalent is prevalent. The equivalent is highly influenced by reactive reserves (generators) hitting their limits. This is also the case for other indices proposed in the literature. Among the data mining methods, DTs are gaining popularity due to their speed, accuracy and system information they provide. In the power system literature, it was found that the work was lacking in a systematic study of attribute selection using power system techniques.

In Chapter 4, to mitigate the influence of generators hitting their limits, the method of reactive reserve allocation has been proposed. This method provides a much better accuracy qualitatively as well as quantitatively compared to the Thévenin equivalent method.. The offline calculation involved is the determination of VCA. The reactive power is allocated to a VCA by calculation of participation factors. The proposed method was applied to 2 bus, 5 bus and the 9 bus systems to demonstrate the idea. Simulations were done on 30 and 118 bus systems to test the effectiveness of the method in large systems.

Chapter 5 presents improvement on decision trees method for online voltage stability monitoring by attribute selection. The role of data mining approach such as decision tree is vital in using the available accurate measurement data in the power system. Also, it is very important to extract important data or attributes so that the tree is robust, reliable and easy to compute. Data mining itself offers information based (gain

ratio), statistical (k-nearest neighbor), probabilistic (naïve Bayes) and others for attribute selection. There are analytical approaches in power systems which can characterize attributes as well. Can these attributes be used for attribute selection for decision trees? The hypothesis has been tested using the tangent vector information of attributes. The test system used was IEEE 30 bus system. It was found for the test case that the accuracy of the selected attributes on decision trees is very high. Attributes with higher sensitivity were found to be better indicators of voltage instability. Attribute selection will be very helpful when it comes to large systems with a huge volume of data.

6.2 Future Work

To improve the accuracy, reliability and speed of voltage stability monitoring using reactive reserves more work needs to be done on error analysis and fast and accurate determination of VCA. This is possible by working on more systems and observing the error behavior. Further, work can be done in the area of techniques to quickly determine the VCA. The proposed method can also be extended to online voltage security assessment by considering a set of credible contingencies and monitoring the smallest margin at any given time.

Regarding selection of attributes for decision trees using power system methods, other methods such as margin sensitivity, modal analysis could be employed to see their performance. Tangent vector method has shown potential (Chapter 5) for the purpose and is recommended for application in more systems to test its reliability. Further, the methods of selection have shown to give weak buses. This is the area that can be further investigated to determine whether the data mining algorithms consistently select attributes related to weak buses.

It is also important that a framework in the control center is such that the final information is based on both types of approaches of stability monitoring: analytical and data mining approaches. As analytical methods can be used to determine attributes, data mining approaches can be used to update system parameters for better analytical study. In this way both the methods complement one another and yield better results. Such a framework is shown in Figure 6.1.

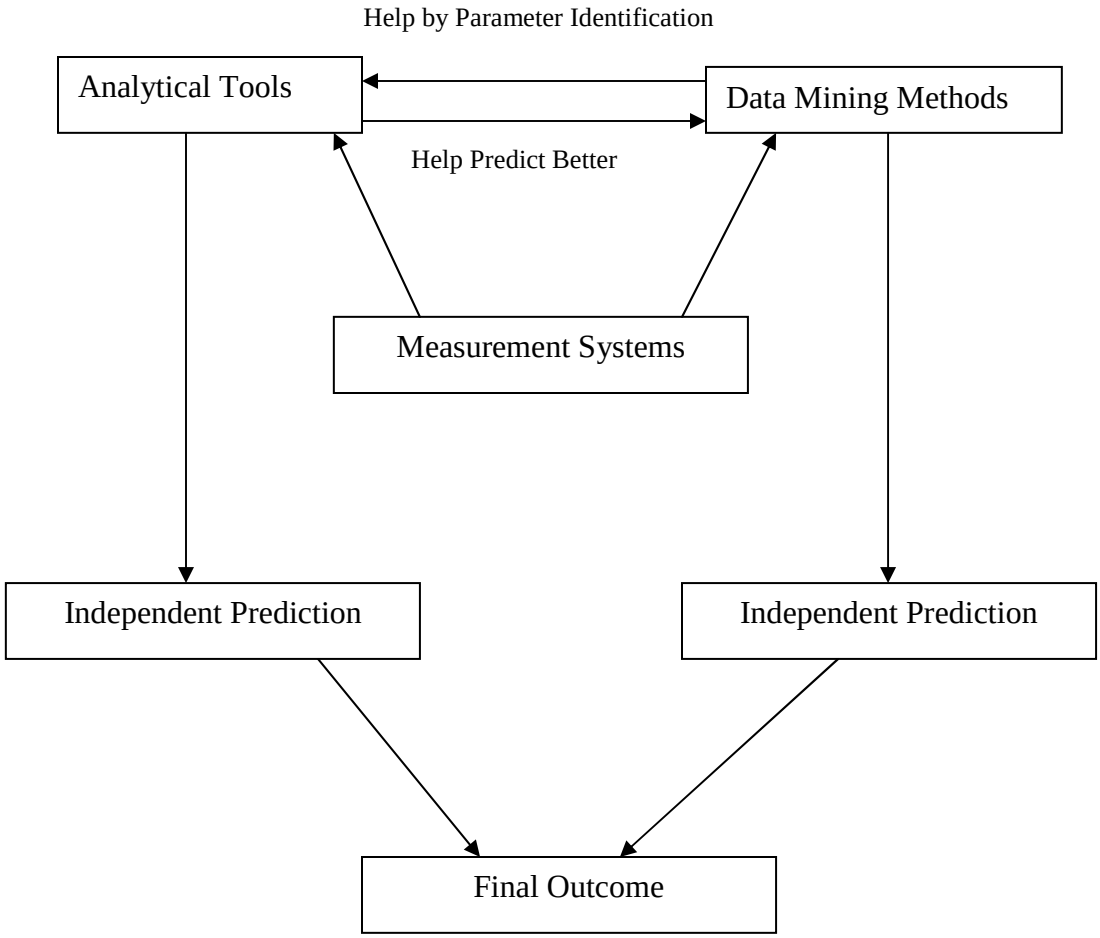

Figure 6.1 Decision tool Using Analytical and Data Mining Tools

APPENDIX A. PARTIAL DATA

This is a partial list of data generated. There are 3450 data points in the entire dataset. ‘V’ indicates voltage and the number associated with it gives the bus number. So, V1 is the column of p.u. voltage magnitudes at bus 1 for the different scenarios. Similarly, ‘A’ stands for angles and the number attached is the bus number.

V1	V2	V3	V4	V5	V6	V7	V8	V9
1	1	0.99	0.99	1	0.99	0.98	1	0.99
1	1	0.99	0.99	1	0.99	0.98	1	1
1	1	0.99	0.99	1	0.99	0.98	1	0.99
1	1	0.99	0.99	1	0.99	0.98	1	0.99
1	1	0.99	0.99	1	0.99	0.98	1	1
1	1	0.99	0.99	1	0.99	0.98	1	0.99
1	1	0.99	0.99	1	0.99	0.98	1	0.99
1	1	0.99	0.99	1	0.99	0.98	1	1
1	1	0.99	0.99	1	0.99	0.98	1	0.99
1	1	0.99	0.98	1	0.99	0.98	1	0.99
1	1	0.99	0.99	1	0.99	0.98	1	1
1	1	0.99	0.99	1	0.99	0.98	1	0.99
1	1	0.99	0.98	1	0.99	0.98	1	0.99
1	1	0.99	0.99	1	0.99	0.98	1	1
1	1	0.99	0.99	1	0.99	0.98	1	0.99
1	1	0.99	0.98	1	0.99	0.98	1	0.99
1	1	0.99	0.99	1	0.99	0.98	1	1
1	1	0.99	0.99	1	0.99	0.98	1	0.99
1	1	0.99	0.98	1	0.99	0.98	1	0.99
1	1	0.99	0.99	1	0.99	0.98	1	1
1	1	0.99	0.99	1	0.99	0.98	1	0.99
1	1	0.99	0.98	1	0.99	0.98	1	0.99
1	1	0.99	0.99	1	0.99	0.98	1	1
1	1	0.99	0.99	1	0.99	0.98	1	0.99
1	1	0.99	0.98	1	0.99	0.98	1	0.99
1	1	0.99	0.99	1	0.99	0.98	1	1
1	1	0.99	0.99	1	0.99	0.98	1	0.99
1	1	0.99	0.99	1	0.99	0.98	1	0.99
1	1	0.99	0.99	1	0.99	0.98	1	1

A23	A24	A25	A26	A27	A28	A29	A30	Pmargin
-18.41	-18.15	-16.59	-16.82	-15.49	-12.6	-15.92	-15.92	insecure
-16.78	-16.49	-15.14	-15.28	-14.21	-12.08	-14.49	-14.48	secure
-17.57	-17.41	-15.94	-16.13	-14.92	-12.37	-15.28	-15.28	alert
-18.23	-18.17	-16.61	-16.84	-15.51	-12.61	-15.94	-15.93	insecure
-16.87	-16.48	-15.13	-15.28	-14.21	-12.07	-14.48	-14.48	secure
-17.68	-17.4	-15.93	-16.13	-14.91	-12.36	-15.27	-15.27	alert
-18.36	-18.16	-16.6	-16.83	-15.5	-12.6	-15.93	-15.92	insecure
-17.17	-16.5	-15.15	-15.29	-14.22	-12.08	-14.5	-14.49	secure
-18.09	-17.43	-15.96	-16.15	-14.94	-12.38	-15.3	-15.29	alert
-18.86	-18.19	-16.63	-16.86	-15.53	-12.62	-15.96	-15.95	insecure
-17.25	-16.51	-15.16	-15.3	-14.23	-12.09	-14.51	-14.5	secure
-18.2	-17.44	-15.98	-16.17	-14.95	-12.39	-15.31	-15.31	alert
-18.99	-18.22	-16.66	-16.89	-15.55	-12.64	-15.98	-15.98	insecure
-17.01	-16.35	-15.04	-15.18	-14.14	-12.06	-14.41	-14.41	secure
-17.89	-17.26	-15.83	-16.02	-14.84	-12.35	-15.19	-15.19	alert
-18.61	-18.01	-16.49	-16.72	-15.42	-12.59	-15.84	-15.84	insecure
-16.88	-16.56	-15.19	-15.34	-14.25	-12.08	-14.53	-14.52	secure
-17.76	-17.5	-16.01	-16.2	-14.97	-12.37	-15.33	-15.33	alert
-18.48	-18.28	-16.69	-16.92	-15.57	-12.61	-16	-15.99	insecure
-16.88	-16.56	-15.19	-15.34	-14.25	-12.08	-14.53	-14.52	secure
-17.76	-17.5	-16.01	-16.2	-14.97	-12.37	-15.33	-15.33	alert
-18.48	-18.28	-16.69	-16.92	-15.57	-12.61	-16	-15.99	insecure
-16.9	-16.58	-15.21	-15.35	-14.26	-12.08	-14.54	-14.54	secure
-17.77	-17.53	-16.03	-16.22	-14.99	-12.37	-15.35	-15.34	alert
-18.5	-18.31	-16.71	-16.94	-15.58	-12.61	-16.01	-16.01	insecure
-16.81	-16.42	-15.09	-15.23	-14.18	-12.07	-14.45	-14.45	secure
-17.65	-17.31	-15.87	-16.06	-14.87	-12.36	-15.23	-15.22	alert
-18.35	-18.05	-16.52	-16.75	-15.44	-12.6	-15.87	-15.87	insecure
-16.64	-16.4	-15.07	-15.22	-14.17	-12.07	-14.44	-14.44	secure

BIBLIOGRAPHY

[1] Joint Task Force on Stability Terms and Definitions, "Definition and Classification of Power System Stability", *IEEE Transactions on Power Systems*, Vol. 19, No.2, May 2004.

[2] T.V. Cutsem, Costas Vournas, *Voltage Stability of Electric Power Systems*. Massachusetts: Kluwer Academic Publishers, 1998.

[3] K. Vu, M. M. Begovic, D. Novosel, M. M. Saha," Use of local measurements to estimate voltage-stability margin," *IEEE Transactions on Power Systems*, vol. 14, pp.1029-35, August 1999.

[4] P.A. Lof, G. Andersson, D.J. Hill, "Fast calculation of a voltage stability index," *IEEE Transactions on Power Systems*, vol.7, no. 1, February 1992.

[5] B. Gao, G.K. Morison, P. Kundur, " Voltage stability evaluation using modal analysis,"*IEEE Transactions on Power Systems*, vol.7, pp.1529-1542, Nov. 1992.

[6] B. Avramovic and L. H. Fink.,"Real-time reactive security monitoring," *IEEE Transactions on Power Systems*, Vol. 7, No. 1, February 1992.

[7] C.W. Taylor, *Power System Voltage Stability*. New York: McGraw-Hill, 1994.

[8] A.G. Phadke, "Synchronized Phasor Measurements in Power Systems**,"** *IEEE Computer Applications in Power*, vol. 6, pp.10 – 15, April 1993.

[9] C.S. Chang, D. Sutanto, W.Lachs, "Automatic control of voltage instability by an expert system utilizing pattern recognition techniques," *Proc. Of the Tenth Power System Computation conference*, Graz, Austria, pp.1057-64, August 1990.

[10] Bansilal, D. Thukaram, K. Parthasarathy, "An expert system for power system voltage stability improvement," *Electrical Power & Energy Systems*, vol. 19, pp.385-392, 1997.

[11] T. Van Cutsem, L. Wehenkel, M. Pavella, B. Heilbornn, M. Goubin, “Decision tree approaches to voltage security assessment,” *IEEE Proceedings-C*, Vol. 140, No. 3, May 1993

[12] R.F. Nuqui, A. G. Phadke, R.P. Schulz, N. Bhatt, “ Fast on-line voltage security monitoring using synchronized phasor measurements and decision trees,” *IEEE PES Winter Power Meeting*, vol. 3, pp. 1347-1352, February 2001.

[13] Ruisheng Diao, Kai Sun, V. Vittal, R.J. O’Keefe, M.R. Richardson, N. Bhatt, D. Stradford, S.K. Sarawagi, “ Decision Tree-Based Online Voltage Security Assessment Using PMU Measurements,” *IEEE Transactions on Power Systems*, vol. 24, pp. 832-839, May 2009.

[14] L. Wehenkel, T. Van Cutsem, M. Pavella, Y. Jacquement, B. Heilbornn, P. Pruvot, “Machine learning, neural networks, and statistical patterns recognition for voltage security: a comparative study,” *Engineering Intelligent Systems*, vol.2, December 1994.

[15] Robert J Schalkoff, *Pattern Recognition: Statistical Structural, and Neural Approaches*, J. Wiley, New York: 1992.

[16] Venkataramana Ajjarapu, *Computational Techniques for Voltage Stability Assessment and Control*, New York: Spring, 2006.

[17] P.W. Sauer and M. A. Pai, “Power system steady-state stability and the load-flow Jacobian”, *IEEE Transactions on Power Systems*, vol.5, no.4, November 1990.

[18] P. Kundur, *Power System Stability and Control.* New York: McGraw-Hill, 1994.

[19] J. Machowski, J. W. Bialek and J. R. Bumby, *Power System Dynamics and Stability*. New York: John Wiley and Sons, 1997.

[20] G.K. Morison, B. Gao and P. Kundur, “Voltage Stability Analysis Using Static and Dynamic Approaches”, *IEEE Transactions in Power Systems*, vol. 8, no. 3, August 1993.

[21] T.E. Dyliacco, “The adaptive reliability control system”, *IEEE Transactions.on Power Apparatus and Systems*, vol. PAS-86, pp.517-531, May 1967.

[22] F. Gubina, B. Strmcnik,"Voltage collapse proximity index determination using voltage phasors approach," *IEEE Transactions on Power Systems*, vol. 10, pp. 788-99, May 1995**.**

[23] F. Gubina, B. Strmcnik, "A simple approach to voltage stability assessment in radial networks,"*IEEE Transactions on Power Systems*, vol.12, pp. 1121-28, August 1997.

[24] L. Fu, B.C. Pal, B.J. Cory, "Phasor measurement application for power system voltage stability monitoring," *IEEE PES Summer Power Meeting*, pp. 1-8, July 2008.

[25] Mats Larsson, Christian Rehtanz, Joachim Berstsch, "Real-time voltage stability assessment of transmission corridors."

[26] M.H. Haque, "Use of V-I Characteristic as a Tool to Assess Static Voltage Stability Limit of a Power System," *IEE Proceedings – Generation, Transmission and Distribution*, Vol. 151, pp. 1-7, 2004.

[27] Borka Milosevic, M. M. Begovic, " Voltage-Stability Protection and Control Using a Wide-Area Network of Phasor Measurements," *IEEE Transactions on Power Systems*, vol.18, no.1, February 2003.

[28] Robert V. Hogg, Elliot A. Tanis, *Probability and Statistical Inference*, New York: Macmillan Publishing Co., Inc. 1983.

[29] V.A. Venikov, V. A. Stroev, V.I. Idelchic, and V.I. Tarasov, "Estimation of electrical power system steady-state stability in load flow calculations," *IEEE Trans. On Power Apparatus and Systems*, vol. PAS-94, pp. 1034-1041, May/June 1975.

[30] P.A. Lof, G. Andersson, D.J. Hill, "Voltage stability indices for stressed power systems," *IEEE Transactions on Power Systems*, vol. 8, Feb. 1993.

[31] C.A. Canizares, A.C.Z. De Souza, V.H. Quintana, " Comparison of performance indices for detection of proximity to voltage collapse," *IEEE Transactions on Power Systems*,vol. 11, pp. 1441-1450, August 1996.

[32] P. Kessel, H. Glavitsch, “Estimating the Voltage Stability of a Power System,” *IEEE Transactions on Power Systems*, vol.1, pp.346-354, July 1986.

[33] V. Galamourougan, T.S. Sidhu, M.S. Sachdev, “ Technique for online prediction of voltage collapse,” *IEE Proceedings- Generation, Transmission and Distribution*, vol. 151, pp. 453-460, July 2004.

[34] R.A. Schlueter, I-P. Hu, M.W. Chang, J. C. Lo, A. Costi, “ Methods for determining proximity to voltage collapse,” *IEEE Transactions on Power Systems*, vol. 6, pp. 285-292, February 1991.

[35] T. Lie, R.A. Schlueter, P.A. Rusche, “Method of identifying weak transmission network stability boundaries,” *IEEE Transactions on Power Systems*, vol.8, pp. 293-301, February 1993.

[36] R.A. Schlueter, “A voltage stability security assessment method,” *IEEE Transactions on Power Systems,*vol. 13,pp. 1423-1438, November 1998.

[37] C. A. Aumuller, T. K. Saha; “Determination of Power System Coherent Bus Groups by Novel Sensitivity-Based Method for Voltage Stability Assessment”, *IEEE Transactions on Power Systems*, Vol. 18, pp. 1157-1164, August 2003.

[38] L. Sandberg, K. Rouden, L. Ekstam, “ Security assessment against voltage collapse based on real-time data including generator reactive capacity,” in CIGRE, 1994, Paper 39/11-03.

[39] W. R. Lachs and D. Sutanto, “Rotor heating as an indicator of system voltage instability,” *IEEE Trans. Power Systems*, vol. 10, pp. 175–181, February 1995.

[40] C. W. Taylor and R. Ramanathan, “BPA reactive power monitoring and control following the August 10, 1996 power failure,” in *Proc. VI Symp. Specialists Elect. Oper. Expansion Planning*, Salvador, Brazil, May 1998.

[41] Lixin Bao, Zhenyu Huang, Wilson Xu, “Online Voltage Stability Monitoring Using VAr Reserves,” *IEEE Transactions on Power Systems*, vol. 18, pp. 1461-1469, November 2003.

[42] J.A. Pecas Lopes, F.M. Fernandas, M.A. Matos, “Fast evaluation of voltage collapse risk using pattern recognition techniques,” *Paper APT 300-20-09 presented at the IEEE/NTUA Athens Power Tech Conference,* Athens, Greece,Sept. 5-8,1993.

[43] David E. Goldberg, *Genetic Algorithms in Search, Optimization, and Machine Learning,* Addison Wesley Longman, Inc., 1989.

[44] Lofti A. Zadeh, *Knowledge representation in fuzzy logic*, Kluwer Academic Publishers, New York, 1992.

[45] Cutsem, T. V. Cutsem, Y. Jacquemart, J.-N. Marquet, P. Pruvot, “A comprehensive analysis of mid-term voltage stability,” IEEE Transactions on Power Systems, vol. 10, pp. 1173-1182, August 1995

[46] M. M. Begovic , A.G. Phadke, “ Dynamic simulation of voltage collapse”, *IEEE Transactions on Power Systems*, vol.5, pp. 1529-1534 ,November 1990

[47] K.T. Vu, C. C. Liu, “Shrinking stability regions and voltage collapse in power systems,” *IEEE Transactions on Power Systems*, vol. 39, pp. 271-289, 1992

[48] Nuqui, R.F. Nuqui, Phadke, A.G. Phadke, “Phasor measurement unit placement techniques for complete and incomplete observability,” *IEEE Transactions on Power Delivery*, vol. 20, pp. 2381-2388, October 2005

[49] A.G. Phadke, J.S. Thorpe, K.J. Karimi, “State estimation with phasor measurements,” *IEEE Transactions on Power Systems*, 1986

[50] I. Smon, G. Verbic, F. Gubina, “Local voltage-stability index using Tellegen’s theorem,” *IEEE Transactions on Power Systems*, vol. 21, pp. 1267-1275, August 2006

[51] S. Corsi, G.N. Taranto, "A real-time voltage instability identification algorithm based on local phasor measurements," *IEEE Transactions on Power Systems*, August 2008

[52] D.E. Julian, R.P. Schulz, K.T. Vu, W.H. Quaintance, N.B. Bhatt, D. Novosel, " Quantifying proximity to voltage collapse using the voltage instability predictor (VIP)," *Proceedings of IEEE PES Summer Meeting*, Seattle, pp. 16-20, July 2000

[53] S. Haykin, *Adaptive Filter Theory*. Upper Saddle River, NJ, USA: Prentice Hall, Inc, 1996

[54] K. Morison, X. Wang, A. Moshref, A. Edris, "Identification of voltage control areas and reactive power reserve; An advancement in on-line voltage security assessment," *Power and Energy Society General Meeting- Conversion and Delivery of Electrical Energy in the 21st Century*, July 2008

[55] "MATPOWER User's Manual", *MATPOWER 3.2 solver* [Online] Available: http://www. pserc.cornell.edu/matpower/

[56] Jiawei Han, Micheline Kamber, *Data Mining: Concepts and Techniques*, San Francisco: Morgan Kaufman Publishers, 2001.

[57] L. Wehenkel, M. Pavella, "Advances in decision trees applied to power system security assessment," *IEE 2nd International Conference on Advances in Power System Control, Operation and Management*, December 1993.

[58] Ian H. Witten, Eibe Frank, *Data Mining: Practical Machine Learning Tools and Techniques with Java Implementations*, San Francisco: Morgan Kaufman Publishers, 2000.

[59] [Online] Available: http://www.cs.waikato.ac.nz/ml/weka/

[60] Michael W. Berry, Murray Browne, *Lecture Notes in Data Mining*. New Jersey, World Scientific Publishing, Co. Pte. Ltd, 2006

ACKNOWLEDGEMENTS

Thanks to Dr. Ajjarapu for his guidance and support in the systematic development of this research. This work wouldn't have been possible without his constant interest and commitment.

Thanks to Dr. Olafsson for his expert advice on implementation of decision trees and use of WEKA software. Thanks to Dr. Aliprantis, Dr. McCalley and Dr. Liu who have been great teachers here at Iowa State in the power systems group.

Thanks to Naresh Acharya for helping me in understanding the logistics of Matpower. He is a very good friend and has encouraged me in my efforts. Thanks to Subhadarshi Sarkar for helping in proofreading the material and being a very good friend. Thanks to Ajay Shah for proofreading the material and suggesting me techniques on technical writing. He is a very good friend. Thanks to other friends at Iowa State and Ames who have been great help when in times of need. Finally, thanks to my family and Sima for being a constant source of motivation.